

# Tempo and mode of evolution across multiple traits in an adaptive radiation of birds (Vangidae)

Anya L.B. Auerbach  <sup>1,2</sup>, Euan Horng Jiunn Lim <sup>1</sup>, Sushma Reddy <sup>2,3</sup>

<sup>1</sup>Department of Ecology, Evolution, and Behavior, University of Minnesota, St. Paul, Minnesota, United States

<sup>2</sup>Bell Museum of Natural History, University of Minnesota, St. Paul, Minnesota, United States

<sup>3</sup>Department of Fisheries, Wildlife, and Conservation Biology, University of Minnesota, St. Paul, Minnesota, United States

Corresponding author: Department of Ecology, Evolution, and Behavior, University of Minnesota, 140 Gortner Laboratory, 1479 Gortner Avenue, St. Paul, MN 55108, United States. Email: [auerb027@umn.edu](mailto:auerb027@umn.edu)

## Abstract

An ongoing challenge in macroevolutionary research is identifying common drivers of diversification amid the complex interplay of many potentially relevant traits, ecological contexts, and intrinsic characteristics of clades. In this study, we used geometric morphometric and phylogenetic comparative methods to evaluate the tempo and mode of morphological evolution in an adaptive radiation of Malagasy birds, the vangas, and their mainland relatives (Aves: Vangidae). The Malagasy radiation is more diverse in both skull and foot shape. However, rather than following the classic “early burst” of diversification, trait evolution accelerated well after their arrival in Madagascar, likely driven by the evolution of new modes of foraging and especially of a few species with highly divergent morphologies. Anatomical regions showed differing evolutionary patterns, and the presence of morphological outliers impacted the results of some analyses, particularly of trait integration and modularity. Our results demonstrate that the adaptive radiation of Malagasy vangas has evolved exceptional ecomorphological diversity along multiple, independent trait axes, mainly driven by a late expansion in niche space due to key innovations. Our findings highlight the evolution of extreme forms as an overlooked feature of adaptive radiation warranting further study.

**Keywords:** adaptive radiation, geometric morphometrics, trait integration, morphological evolution, birds

## Introduction

Adaptive radiations—clades that have undergone an exceptional degree of ecological diversification—are emblematic examples of evolution and offer powerful opportunities to help understand the processes that generate ecological and phenotypic diversity (Givnish & Sytsma, 1997; Hedges & Dierieg, 2009; Schlüter, 2000). Despite substantial interest in the study of adaptive radiation, major disagreements remain regarding (1) how these clades should be identified and (2) the generalizability and predictive power of these patterns as evolutionary models (Gavrilets & Losos, 2009; Losos & Miles, 2002; Moen et al., 2021; Olson & Arroyo-Santos, 2009). Many shared general patterns have been proposed for adaptive radiations, but most are not generalizable across the diversity of clades usually considered under this framework, making identification of radiations and their comparative study difficult (Gillespie et al., 2020). Also poorly understood is the degree to which adaptive radiation is predictable, in terms of both the external factors and intrinsic features of clades that may promote or inhibit radiation (De-Kayne et al., 2024; Glor, 2010; Kassen, 2009; Losos & Mahler, 2010; Lovette et al., 2002; Stroud & Losos, 2016; Wellborn & Langerhans, 2015; Yang, 2001). Although many studies have examined rates of evolutionary change in radiations, understanding their predictability will require reconciling variable patterns of diversification across

multiple traits, which may be subject to different selective pressures.

One of the most common patterns used to identify adaptive radiation is an “early burst”—but an overemphasis on this criterion risks obscuring the true complexity of macroevolutionary processes by excluding other modes of diversification. The early burst has often been considered a defining feature because classically, adaptive radiations are predicted to undergo rapid early diversification in response to some ecological opportunity, followed by declining rates of diversification as niche space is filled (Freckleton & Harvey, 2006; Gavrilets & Losos, 2009; Martin & Richards, 2019; Schlüter, 2000; Simpson, 1944). Until recently, the emphasis on testing for an early burst resulted in a focus on speciation rates, while the importance of quantifying ecological diversity was often overlooked (Givnish, 2015; Yoder et al., 2010). More recently, methodological advances have enabled a shift toward testing for an early burst using trait data and other measures of ecological diversity (Harmon et al., 2010; Mahler et al., 2010; Slater et al., 2010). These studies have revealed that, while rapid speciation appears to be correlated with ecological trait diversification on average (Cooney & Thomas, 2021; Rabosky et al., 2013), these processes are frequently decoupled in individual clades (Barreto et al., 2023; Derryberry et al., 2011; Folk et al., 2019; Martin & Richards, 2019; Reaney et al., 2020; Rowsey et al., 2019; Venditti et al., 2011). Furthermore, the framework of

Received December 16, 2024; revisions received May 12, 2025; accepted May 26, 2025

Associate Editor: Emma Sherratt; Handling Editor: Hélène Morlon

© The Author(s) 2025. Published by Oxford University Press on behalf of The Society for the Study of Evolution (SSE). This is an Open Access article distributed under the terms of the Creative Commons Attribution-NonCommercial License (<https://creativecommons.org/licenses/by-nc/4.0/>), which permits non-commercial re-use, distribution, and reproduction in any medium, provided the original work is properly cited. For commercial re-use, please contact [reprints@oup.com](mailto:reprints@oup.com) for reprints and translation rights for reprints. All other permissions can be obtained through our RightsLink service via the Permissions link on the article page on our site—for further information please contact [journals.permissions@oup.com](mailto:journals.permissions@oup.com)

comparing support for a limited set of diversification scenarios (e.g., early burst vs. Brownian motion) can lead to misidentification of other, often more complex models (Martin et al., 2023). Although an early burst can be a strong indicator of diversification in response to ecological opportunity, defining adaptive radiation solely by this criterion has the potential to limit our understanding of how different conditions may impact the tempo of diversification (Astudillo-Clavijo et al., 2015; Losos & Mahler, 2010).

Identifying appropriate ecologically relevant traits to target for a given clade is itself an ongoing challenge. Many studies focus on single, univariate measurements such as body size, despite conceptual models of adaptive radiation that often involve simultaneous and/or sequential divergence in multiple aspects of adaptive changes (Slater, 2022). The results from any single trait risk being fundamentally misleading if diversification has occurred along multiple trait axes. The appropriate selection of traits for a particular clade, and how to consider simultaneous or sequential diversification of multiple traits, is increasingly being recognized as a critical component of macroevolutionary research (Ackerly et al., 2006; Donoghue & Sanderson, 2015; Grossnickle et al., 2024; Guillerme et al., 2020; Mutumi et al., 2023; Slater & Friscia, 2019). Examining a variety of traits will best represent the underlying ecological diversity present in different clades, and this attention to organismal biology and natural history knowledge remains essential for drawing robust conclusions (Losos, 2010). Different ecologically relevant traits may show different patterns of diversification in the same clade, as in the Malagasy radiation of mantellid frogs, where evolutionary rates of shape but not size or performance-related metrics were elevated relative to other anuran clades (Moen et al., 2021). We should expect adaptive radiation to frequently proceed along multiple axes of diversification, and in these cases, understanding the evolutionary dynamics of these traits in concert is central to understanding how diversity is generated.

Another major area of evolutionary research concerns understanding variation in the intrinsic capacity of a clade to diversify, i.e., its evolvability. Several factors have been proposed to explain why, even when seemingly presented with similar ecological opportunity, some clades diversify so spectacularly, whereas others do not (Jablonski, 2022; Lovette et al., 2002; Sidlauskas, 2008; Wellborn & Langerhans, 2015). A key characteristic impacting evolvability is the degree of independence between components of an organism's phenotype (Jablonski, 2022; Kirschner & Gerhart, 1998; Yang, 2001). Traits less able to vary independently of one another are described as more integrated, whereas modularity refers to the organization of traits into discrete "quasi-independent" regions (modules). Integration and modularity impact evolutionary rates and trajectories at multiple levels—genetic, developmental, and evolutionary (Cheverud, 1984; Conith et al., 2021; Klingenberg, 2008; Schlüter, 1996; Zelditch & Goswami, 2021). We focus here on evolutionary integration as measured by comparing patterns of morphological trait covariation across a clade.

Theoretical and empirical studies have shown mixed evidence for how integration and modularity may shape adaptive radiations. Higher modularity has usually been thought to promote evolvability, with greater trait independence permitting a wider range of phenotypes to evolve (Dellinger et al., 2019; Felice & Goswami, 2018; Larouche et al., 2018;

Wagner & Altenberg, 1996; Walter et al., 2018; Yang, 2001). However, other studies suggest that integration can facilitate the evolution of more disparate phenotypes by maintaining key functional relationships and promoting rapid evolution along paths of least resistance (Evans et al., 2021; Goswami et al., 2014; Griswold, 2006; Hedrick et al., 2020; Navalón et al., 2020; Schlüter, 1996). Continued work to uncover how integration and modularity shape rates and patterns of trait evolution is necessary to begin to understand the wide variation in evolvability we observe across clades (Felice et al., 2018; Troyer et al., 2024).

The adaptive radiation of Malagasy vangas is an ideal system in which to explore these questions regarding the tempo and mode of morphological diversification. The 40-odd species in the family Vangidae are shrike-like birds widespread in tropical Africa and Asia, but slightly over half belong to a monophyletic subfamily endemic to Madagascar (Vanginae) (Clements et al., 2023; Reddy et al., 2012). The Malagasy Vanginae have diversified into a spectacular array of forms, misleading early taxonomists who initially classified them as members of numerous other bird families (Johansson et al., 2008; Reddy et al., 2012; Yamagishi et al., 2001). Vangas are understudied relative to other avian radiations, notably the Galapagos finches and Hawaiian honeycreepers, and differ significantly from these clades in many aspects of natural history. Vangas are all insectivores (some incorporating vertebrate prey), and have diversified primarily in terms of foraging strategy rather than diet: Different species employ a variety of maneuvers that can be broadly categorized as gleaning, sallying, and probing, with corresponding morphological specializations (Reddy & Schulenberg, 2022; Yamagishi & Eguchi, 1996). This niche partitioning has enabled an exceptional degree of sympatry, with about 15 species co-occurring in rainforest communities (Wilmé, 1996).

An exceptional feature of the Malagasy vanga radiation is the presence of a handful of taxa that have evolved especially divergent and sometimes unusual morphologies associated with specialized foraging strategies. Examples include the extremely long, decurved bill of *Falculea palliata*, specialized for probing in cavities in search of prey; the massive, deep, and strongly hooked bill of the sallying predator *Euryceros prevostii*; and modified foot proportions in the terrestrial *Mystacornis crossleyi* and nuthatch-like, tree-creeping *Hypositta corallirostris* (Johansson et al., 2008; Reddy & Schulenberg, 2022). The presence of such extremes is a fundamental component of the radiation, but also has the potential to disproportionately drive signal or alter the results of analyses.

Prior studies that examined diversification of the Malagasy vangas found speciation rates largely consistent with the classic model of an early burst following ecological opportunity (Jönsson et al., 2012; Reddy et al., 2012). Using standard linear measurements of bill and body, Jönsson et al. (2012) found that relative trait disparity also fit an early burst, but detected a marginal secondary burst in both relative disparity and speciation rate corresponding to the origin of derived "probing" foraging behaviors.

In this study, we examined patterns of morphological diversification in the Vangidae, focusing on anatomical regions closely tied to foraging behavior: the bill, neurocranium, and feet. The bill is the ecomorphological trait most frequently studied in birds, being closely tied to diet and

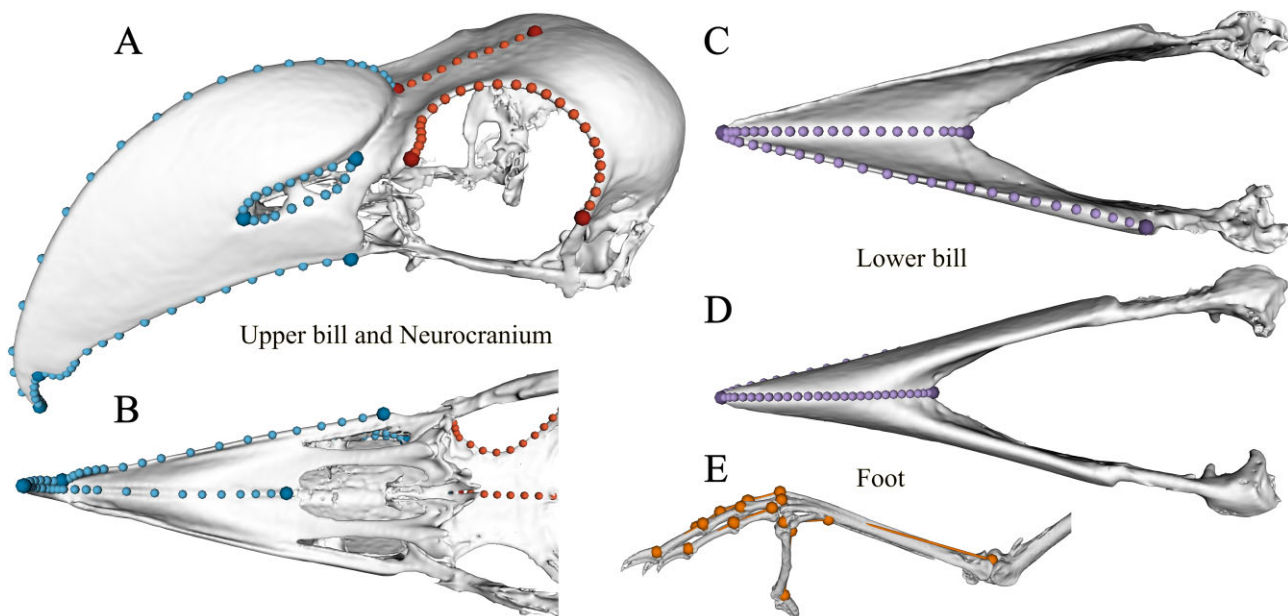


**Figure 1.** Three-dimensional landmark configurations and linear measurements of pedal bones used in this study. Stationary landmarks are shown as larger, darker points, most located at the end of each semilandmark curve. Left: (A) dorsolateral and (B) ventral view of the upper bill (with points in blue) and neurocranium (red). Right: (C) dorsal and (D) ventral view of the lower bill (purple), and (E) linear measurements were taken between each pair of points on the pedal bones (orange).

foraging behavior (Cooney et al., 2017; Dehling et al., 2016; Krishnan, 2023; Mosleh et al., 2023; Pigot et al., 2016; Zusi, 1993), while cranial features reflect variation in musculature, vision, and neuroanatomy (Eliason et al., 2021; Navalón et al., 2020; van der Meij & Bout, 2008). Avian pedal morphology is far less studied, although the diversity of hindlimb anatomy in birds has known relationships to locomotory mode (Abourachid et al., 2017; Dickinson et al., 2023; Falk et al., 2021; Miles & Ricklefs, 1984). We used a range of geometric morphometric and phylogenetic comparative methods to explore the tempo and mode of morphological evolution in vangas and address several fundamental questions in the study of adaptive radiation. We took a comparative approach, contrasting the radiation of Malagasy vangas with the rest of the Vangidae, to evaluate the degree to which ecological opportunity in Madagascar has facilitated exceptional trait diversification. First, we assessed whether overall morphological disparity is in fact higher in the Malagasy clade than in their mainland relatives. Second, we asked whether stronger integration or modularity is associated with morphological diversification across the family. Third, we examined how rates of evolution have varied through time across Vangidae. Throughout, we evaluated how including multiple anatomical traits shifts our view of diversification patterns and assessed the evidence for correlated evolution. We also sought to evaluate the role of extremely divergent morphologies in driving our analyses of trait diversification.

## Methods

### Data collection

We obtained morphometric data from microCT scans of museum specimens, both alcohol-preserved (fluid) whole specimens and stuffed round skins. These specimen types were

required because they preserve the rhamphotheca, the keratinous sheath that interacts directly with the environment (Chhaya et al., 2023; Cooney et al., 2017; Eliason et al., 2020). Fluid specimens were preferred because the entire body is preserved, but to improve our taxonomic sampling, we included round skins, which contain only partial skeletons (usually the anterodorsal portion of the skull and distal portions of the limbs). Specimen and scan details can be found in [Supplementary Table S1](#), and all CT scans used in this study are available on MorphoSource. In total, we obtained scans of 75 specimens, with most species represented by more than one specimen. Our morphometric dataset included all genera and 34 of the 41 recognized species of Vangidae (Clements et al., 2023; Younger et al., 2019), though we were only able to obtain foot measurements for 30 species. Body mass was taken from the AVONET dataset (Tobias et al., 2022) except for *Scetophaga rufa occidentalis*, which was found in Safford and Hawkins (2013).

We segmented each scan using 3D Slicer V4.11 (Fedorov et al., 2012; 3D Slicer, 2020), then cleaned and smoothed all meshes in Autodesk Meshmixer V3.5 (Autodesk Inc., 2018), and placed landmarks on each module in Stratovan Checkpoint (Stratovan Corporation, 2018). Our landmark dataset consists of 214 landmarks, including 13 stationary landmarks and 9 curves (Figure 1, [Supplementary Table S2](#); see Supplemental Methods for further details). We placed landmarks only on the left side to avoid unnecessarily increasing the dimensionality of the data (Cardini, 2017). For the hindlimbs, we used 3D Slicer to digitally measure the lengths of 12 bones from one foot of each specimen: the tarsometatarsus, first metatarsal, and all but the ultimate (ungual) phalanges of each digit (Figure 1, [Supplementary Table S2](#)). All data and code required to reproduce all of our analyses have been deposited on Dryad.

All morphometric analyses were performed in R version 4.3.0. Landmarks were aligned using a generalized

Procrustes analysis (GPA) in *geomorph* version 4.0.7 (Adams et al., 2024; Baken et al., 2021; Gower, 1975; Rohlf & Slice, 1990); semilandmark curves were slid to minimize bending energy (Bookstein, 1997). We mirrored the left-side-only landmarks using the mirrorfill function in *paleomorph* version 0.1.4 prior to performing the GPA, then deleted the mirrored landmarks (Cardini, 2017; Lucas & Goswami, 2017). The lengths of hindlimb bones were transformed into log-shape variables by dividing by the geometric mean and then taking the natural log of that ratio, following, e.g., Slater (2022) and Roberts-Hughes et al. (2023).

We were unable to quantitatively account for the influence of intraspecific variance or measurement error because of small sample sizes due to specimen and time limitations. Both factors can decrease phylogenetic signal and therefore increase support for more complex models, in particular, elevated recent trait diversification rates (Cooper et al., 2016; Silvestro et al., 2015). To confirm qualitatively that intraspecific variation is fairly small relative to the magnitude of trait divergence across vangas, we visualized variation of all specimens using a principal component analysis (PCA) to ensure that conspecifics clustered together (Supplementary Figure S1) and then averaged landmark coordinates by species for all subsequent analyses.

Our morphological dataset was comprised of four anatomical modules, which we used for all analyses: upper bill, lower bill, neurocranium, and feet (Figure 1). The skull modules (bill and neurocranium) are functionally and structurally discrete, and are consistent with prior work that identified the major modules of the avian skull (Felice & Goswami, 2018), although the lower bill was not included in that study. We performed a separate GPA on each module to avoid averaging variance across modules, a particular concern when some regions project far from the center of the shape, as with bird bills (Cardini, 2019; Cardini & Marco, 2022).

We used a time-calibrated phylogeny of the Vangidae produced using reduced-representation genomic data targeting ultraconserved elements (UCEs; in preparation). In brief, this analysis included all described species of the family Vangidae except for 5 species outside of Madagascar (78 taxa total). Given the high variability of phylogenetically informative sites in UCE loci, which can exacerbate divergence dating analyses, we pruned our dataset to include only the 1,000 most informative loci (following Chen et al. 2021) and then randomly subsampled 100 loci to create 10 subsets. For each subset, we ran an entropy estimation script to identify regions with differential rates of evolution (i.e., conserved cores vs. variable flanking regions) and used PartitionFinder 2 (Lanfear et al., 2017) to identify sets of loci with similar rates that can be combined in our model estimates. In BEAST 2.5 (Bouckaert et al., 2019), we conducted analyses of each subset for 100 million generations using a fixed topology from our maximum likelihood analyses and calculating branch lengths to estimate divergence times using the partition scheme and model settings from the PartitionFinder results. We used calibration estimates from Claramunt and Cracraft (2015), which used the largest set of verified fossils to date, to fix the most recent common ancestor of the root (Vangidae + Platystyridae) as 27.36 Ma (95% highest posterior density 22.71–32.09). We compared our resulting divergence times with those of other recent analy-

ses of passerines (Oliveros et al., 2019) and found them to be comparable and within the 95% confidence intervals.

### Patterns of morphological disparity

To visualize the major axes of shape variation in vangas, we performed PCAs on the GPA-aligned landmarks and log-shape variables using the gm.prcomp function in *geomorph*. We used standard, rather than phylogenetic, PCA, as this results in strictly orthogonal axes, which are required as input for several downstream analyses (Polly et al., 2013; Revell, 2009). We performed separate PCAs on each module and on the combined landmark dataset to assess how overall patterns of variation differed between anatomical regions.

Initial exploratory analyses identified several Malagasy taxa as extreme outliers in each module (see the *Results* section; Figure 2, Table 1). To visualize the effect of these outliers on the primary axes of variation, we performed additional PCAs in which we initially excluded the outlier taxa. The outliers were then projected into the ordination by multiplying their GPA-aligned landmark configurations or mean-centered log-shape variables by the eigenvectors from the initial PCA; this is referred to as a post hoc rotation. Most subsequent analyses were performed on both the full set of Malagasy vangas and with either one or two outliers excluded to assess the degree to which our results were driven by the presence of these extreme morphologies.

To quantify differences in disparity between the Malagasy and non-Malagasy vangas and between foraging categories, we used kernel density hypervolumes, overall disparity (based on Procrustes variance), and multivariate analysis of variance (MANOVA; Adams, 2014a; Blonder et al., 2018; Zelditch et al., 2012). Foraging categories follow Reddy et al. (2012). Kernel density hypervolumes have the benefit of accounting for the presence of holes in the morphospace, such as those created by outliers, but are limited by the hypervolume space becoming sparse as the dimensionality of the data increases (Blonder, 2016). On the other hand, overall disparity does not account for holes in morphospace but has the benefit of using the full dimensionality of the dataset. We also estimated the degree of phylogenetic signal for each module, and compared its strength both between clades and between modules, to evaluate the degree to which disparity could be explained by evolutionary relatedness (Collyer & Adams, 2018, 2024; Collyer et al., 2022). Details of these analyses are described in the Supplemental Methods.

### Integration and modularity

The degree of integration can be quantified both within and between anatomical modules, and these quantities together relate to modularity, often measured as the ratio of within-module to between-module integration. For each analysis, we calculated the strength of integration or modularity for each module or pair of modules, then compared this value between clades. We also assessed the impact of anatomical outliers on observed clade-wide patterns of trait covariation by removing them from the dataset one at a time as well as together for each analysis.

We calculated within-module integration as the relative eigenvalue index (Conaway & Adams, 2022; Pavlicev et al., 2009). We calculated integration between modules using a phylogenetic partial least-squares analysis (Adams & Collyer, 2016; Adams & Felice, 2014; Bookstein et

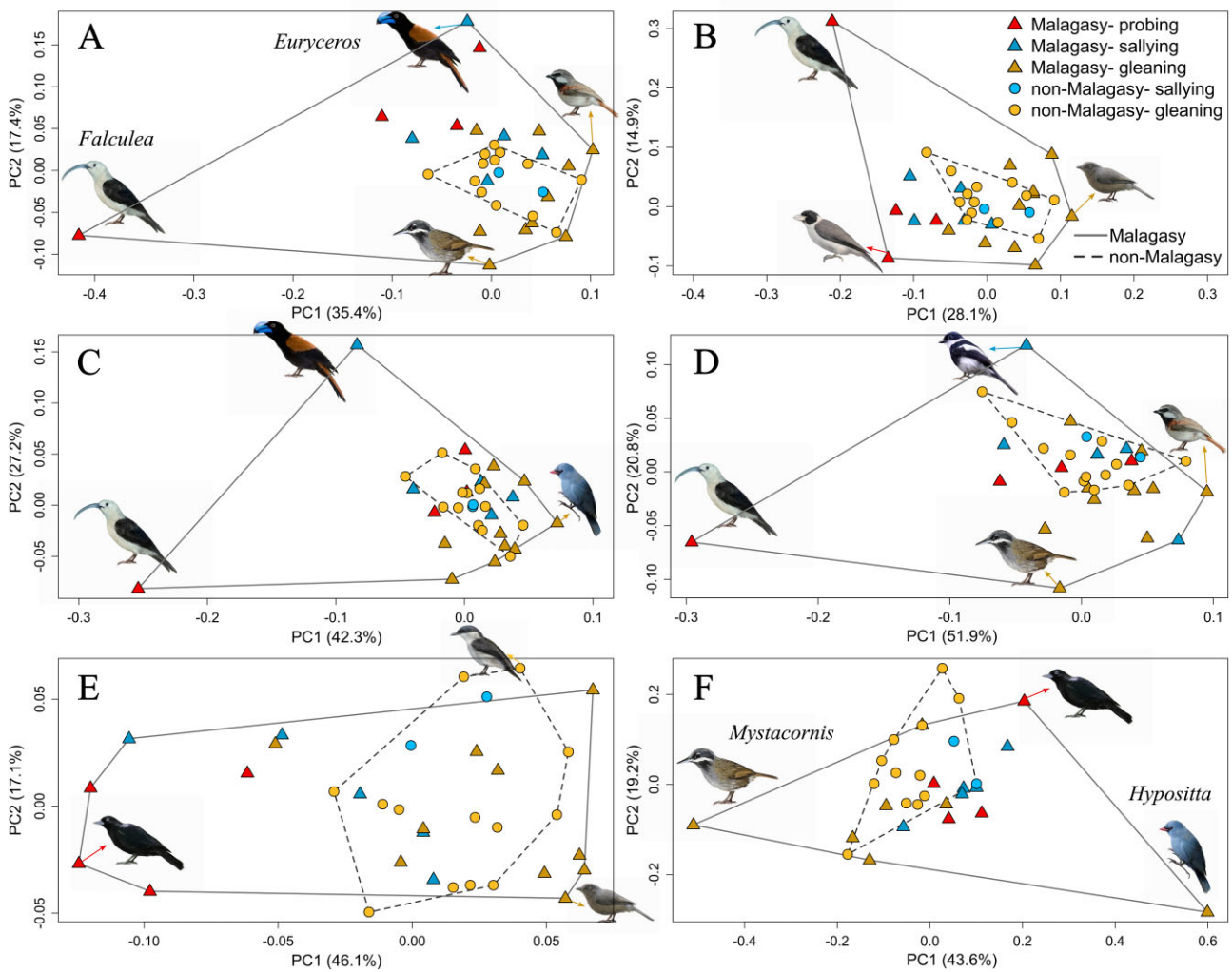


**Figure 2.** Morphological diversity in vangas. Principal components 1 and 2 from PCAs of generalized Procrustes analysis (GPA)-aligned landmark configurations for the skull and log-shape variables for the feet. Top row: (A) whole skull and (B) whole skull post hoc rotation scores, showing differences in the primary axes of variance when outliers are excluded. Middle: (C) upper bill and (D) lower bill. Bottom: (E) neurocranium and (F) feet. Triangles represent Malagasy vangas, while circles represent non-Malagasy vangas. Points are colored by foraging category, with red for probing, blue for sallying, and yellow for gleaning; darker shades are used for the Malagasy vangas. Convex hulls are drawn around each clade, solid (Malagasy) and dashed (non-Malagasy). Inset birds represent the extremes of shape; outliers are labeled. Illustrations of birds by Velizar Simeonovski.

**Table 1.** Morphological diversity of the Malagasy vs. non-Malagasy vangas by anatomical region.

Module	Outliers	Hypervolumes		Disparity		MANOVAs	
		Fold difference	Fraction unique <sup>a</sup>	Phylogenetic	Non-phylogenetic		
Upper bill	<i>Falculea</i> , <i>Euryceros</i>	<0.002 (10.247)	0.004	0.101	0.773	0.243	
Lower bill	<i>Falculea</i>	0.040 (4.862)	0.028	0.073	0.714	0.416	
Neurocranium	–	0.048 (2.104)	0.048	0.096	0.678	0.083	
Whole skull	<i>Falculea</i> , <i>Euryceros</i>	0.004 (10.758)	0.006	0.045	0.752	0.179	
Skull (post hoc)	<i>Falculea</i>	0.012 (8.227)	0.002	–	–	–	
Skull (no outliers)	–	0.010 (5.361)	<0.002	0.040	0.158	0.136	
Feet	<i>Mystacornis</i> , <i>Hypositta</i>	0.076 (3.933)	0.022	0.149	0.785	0.019	
Feet (post hoc)	–	0.202 (2.379)	<0.002	–	–	–	

<sup>a</sup>Fraction unique for Malagasy; for non-Malagasy vangas, fraction unique did not approach significance except for the foot post hoc rotation scores ( $p = 0.046$ ).

Note. Significance of differences in morphological diversity between clades (p values), quantified using kernel density hypervolumes from the first three PC axes for each module, and disparity and MANOVAs (multivariate analysis of variance) from the full landmark or linear measurement dataset. Outliers are identified from PC axes. Fold difference is the magnitude of difference in hypervolume size (magnitude of fold difference reported in parentheses); fraction unique is the percentage of hypervolume unique to the subclade. Significant differences are bolded.

al., 2003) and modularity as the covariance ratio (Adams, 2016; Adams & Collyer, 2019). Details of all analyses may be found in the Supplemental Methods. We focused our analyses of between-module integration and modularity on the adjacent pairs of skull modules (upper bill and skull, upper and lower bills) but also tested for integration between each skull module and the feet.

### Evolutionary rate analyses

The complexity of shape variation in vangas meant that a multivariate approach was necessary to accurately assess rates of morphological evolution, and our hypotheses required evaluating how rates have varied across branches of the vanga tree. Currently available methods for analyzing high-dimensional trait datasets (e.g., Clavel & Morlon, 2020; Clavel et al., 2019) have not yet been developed for models with heterogeneous evolutionary rates, making dimensionality reduction necessary. We used BayesTraits v4.0 (Pagel et al., 2022; Venditti et al., 2011) to assess shifts in rates of morphological evolution across Vangidae. Following common practice (Evans et al., 2021; Felice & Goswami, 2018), we used as our trait data principal component axes summarizing 95% of total shape variation, as the first few axes will tend to bias results toward detecting an early burst (Uyeda et al., 2015); see Miller et al. (2025) for further discussion of the benefits and limitations of this type of approach. PC scores for BayesTraits input were multiplied by 1,000 to avoid computational issues that arise from small numbers in BayesTraits (Troyer et al., 2024). We compared the fit of a series of local tree transforms using five different scaling parameters, termed kappa, lambda, delta, node, and branch. Kappa, lambda, and delta transforms rescale overall relative branch lengths, while node and branch transforms indicate a shift in either the rate or mean value of the trait for the descendant clade (Pagel, 1999; Pagel et al., 2022; see Supplemental Methods for details). For each transform, we tested the fit of three rate shift placements: (1) at the root of the Malagasy clade (equivalent to early burst); (2) at the root of the “derived” clade of foraging behaviors; and (3) multiple shifts occurring elsewhere on the phylogeny. For the first two, we specified the node at which the transform would occur using the *LocalTransform* command. For the third, we used a reversible-jump Markov chain Monte Carlo (rjMCMC) approach (*RJLocalTransform* option in BayesTraits) to determine for each transform the location and number of shifts that best fit the data. Finally, we implemented the “Fabric” model (Pagel et al., 2022), which uses rjMCMC to simultaneously detect directional (branch transform) and evolutionary rate changes (node transform). See Supplemental Methods and **Supplementary Table S9** for a complete list of all tested models and model settings.

We used these models to evaluate the tempo and mode of evolution in a total of five trait datasets: whole skull, whole skull with post hoc rotation, bill (upper + lower), feet, and body mass. Dimensionality reduction to 95% of total variation resulted in 13 PC axes for the skull dataset, 14 for the skull with post hoc rotation, 9 for the bill, and 7 for the feet. For each model, we ran five independent Markov chains and compared the fit of each model to a null model of constant rates using Bayes factors from a stepping-stone sampler; see Supplemental Methods for details.

As a complementary means of understanding the rate of trait diversification through time, we performed a disparity-through-time analysis on each trait dataset using the function *dtt* in the R package *geiger* version 2.0.11 (Harmon et al., 2003; Pennell et al., 2014; Slater et al., 2010; see Supplemental Methods for details).

We also compared the net rates of morphological evolution between the Malagasy and non-Malagasy vangas and between foraging modes using the *compare.evol.rates* function in *geomorph* (Adams, 2014b; Denton & Adams, 2015). This analysis finds the net rate of evolution under a Brownian motion (BM) model and calculates the ratio of rates for two or more groups. Both permutation- and simulation-based methods are available for assessing the significance of the rate ratio; we evaluated the results of both options (Adams & Collyer, 2018).

## Results

### Patterns of morphological disparity

Our analyses confirmed that Malagasy vangas are much more morphologically diverse in the measured traits than non-Malagasy vangas. PCAs (Figure 2) show that across all four modules, the Malagasy vangas occupy a far greater total spread of morphospace along the primary axes of variance. As expected, some species with extreme morphologies appear as outliers and drive much of the variation seen on PC1 and PC2 (Figure 2). *Falculea* (Sickle-billed Vanga) is highly divergent in both upper and lower bill shape (Figure 2C, D), while *Euryceros* (Helmet Vanga) is an outlier in upper bill only. In the feet, *Mystacornis* (Crossley’s Vanga) and *Hypositta* (Nuthatch-Vanga) were outliers, with the difference between them defining the primary axis of variation (Figure 2F). *Mystacornis* has a proportionally elongated tarsometatarsus and shortened hallux, whereas the reverse is true in *Hypositta*. Although the Malagasy vangas were more diverse than the non-Malagasy vangas in neurocranial shape, no taxa were outliers (Figure 2E). The Malagasy vangas also occupied a greater region of morphospace on subsequent PC axes (Supplementary Figure S2).

PCAs with post hoc rotation of these outliers showed that they did substantially alter the loadings of variables on the primary axes of variance, changing the general patterns that emerged for the clades as a whole (Figure 2B, Supplementary Figures S2 and S3). Notably, *Falculea* remained an outlier, albeit more on PC2 than PC1, but *Euryceros* is in the middle of the space. To evaluate the role these outliers play in driving the overall disparity of the Malagasy radiation, for each test of disparity, we compared the Malagasy vangas as a whole, the Malagasy vangas with outliers removed, the Malagasy vangas using post hoc rotation scores (where relevant), and the non-Malagasy vangas.

Malagasy and non-Malagasy vangas differed in disparity, mean shape, or both for all measured traits (Table 1). Our analyses of morphospace hypervolumes found that the Malagasy vangas occupied significantly more morphospace than the non-Malagasy vangas for all skull modules, but not the feet, and that a significant fraction of the morphospace was unique to the Malagasy vangas for all trait datasets (Table 1, Figures 3 and Supplementary Figure S4). Overall disparity was always greater in the Malagasy vangas, but differences were only significant for the whole skull (Table 1). MANOVAs indicated that average shape was

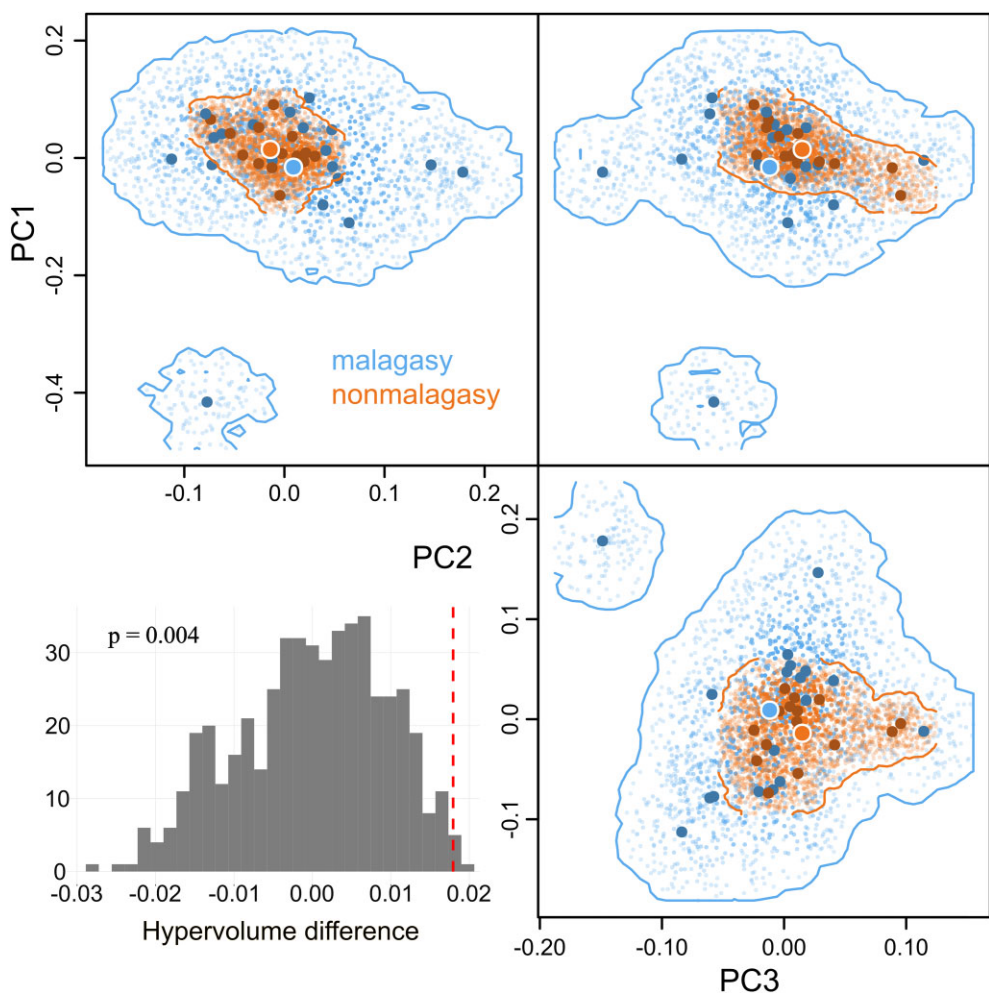


**Figure 3.** Morphospace hypervolumes of the skull for Malagasy (blue) and non-Malagasy (orange) vangas. Hypervolumes are for the first three PC axes from the whole skull landmark dataset. Large, dark points represent the observed point for each species, and the small points represent the density distribution of the hypervolume. The two largest points with white borders indicate the centroid of each clade. The inset histogram is the null distribution of hypervolume differences from the permutation test, with a dashed line indicating the observed difference in volume.

significantly different between the clades only for the feet (Table 1); ANOVAs of each pedal bone indicated that these differences are spread across the first three digits (Supplementary Table S3).

Vangas in the three foraging categories occupy distinct regions of morphospace and differ in their degree of overall morphological disparity. In the whole skull and neurocranium, gleaners and probers do not overlap on the first two PC axes, with salliers occupying an intermediate position (Figure 2). MANOVAs but not phylogenetic MANOVAs found that these differences in overall shape were significant for all skull modules, with probers consistently showing greater disparity than the other foraging classes (Supplementary Table S4). For foot shape, gleaners dominate the primary PC axes because both outliers are in this category (Figure 2). Foraging classes were also significantly different in mean foot shape, though not in disparity, but only when analyzed using post hoc rotation scores (Supplementary Figure S3, Supplementary Table S4).

We detected significant phylogenetic signal for most modules and subclades, and differences between categories were nearly all statistically significant (Supplementary Table S5). Notably, phylogenetic signal in the non-Malagasy vangas

was highest in the upper bill, whereas in the Malagasy vangas, it was highest in the neurocranium, with no significant signal in the upper bill except when both outliers were excluded.

#### Integration and modularity

Within-block integration (eigenvalue dispersion) was consistently but not significantly higher in the Malagasy vangas across modules (Supplementary Table S6). Removing both *Falculea* and *Euryceros* from the Malagasy dataset always decreased integration in the remaining Malagasy vangas, usually below that of the non-Malagasy clade.

The upper bill and neurocranium were more integrated in the Malagasy vangas, while the upper and lower bills were more integrated in the non-Malagasy vangas; however, in both comparisons, removing the outliers reversed this pattern (Supplementary Table S7). Plotting the scores from the first axes of covariance revealed that both *Euryceros* and *Falculea* deviate massively from the dominant patterns of covariance for the rest of the clade (Figure 4). As with eigenvalue dispersion, few differences were statistically significant. For the upper bill and neurocranium, removing both outliers left the remaining Malagasy vangas with no signifi-

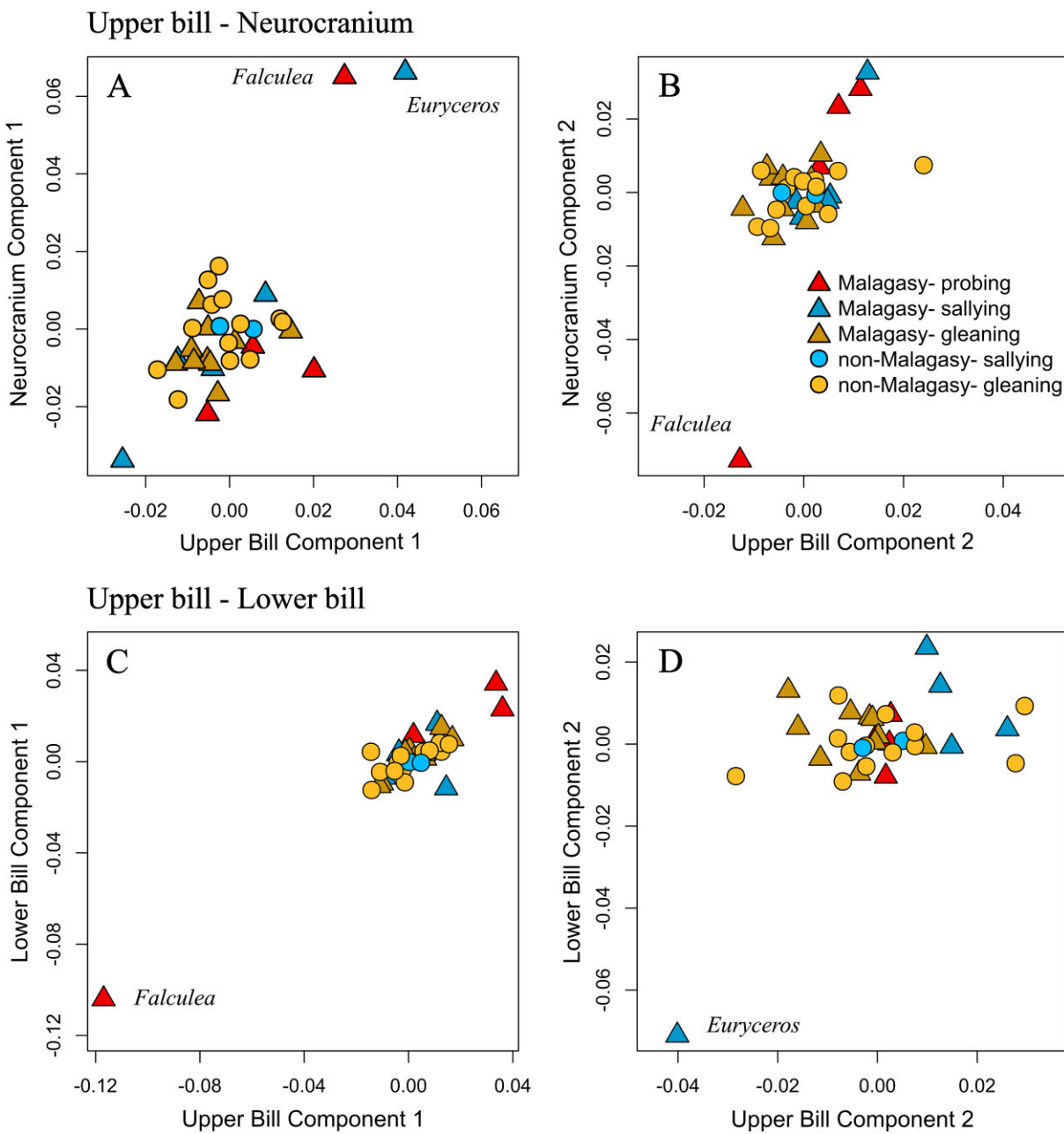


**Figure 4.** Skull shape integration in vangas. Scores from the first two pairs of partial least-squares analysis axes testing integration of the upper bill and neurocranium (top) and upper and lower bills (bottom). These are similar to PCA plots, but show the primary axes of mutually predictive variance for each pair of anatomical modules. Partial least-squares analysis components 1 (A, C) and 2 (B, D). Triangles represent Malagasy vangas, while circles represent non-Malagasy vangas. The points are colored by foraging category, with red for probing, blue for sallying, and yellow for gleaning; darker shades are used for the Malagasy vangas. The positions of anatomical outliers (*Euryceros*, blue and *Falculea*, red) are indicated on each plot.

cant integration; including *Euryceros* appeared necessary to make these modules significantly integrated (Supplementary Table S7). The bill was most strongly integrated when both outliers were removed, and not significantly integrated at all when only *Falculea* was removed, though none of these differences were significant. The feet were not significantly integrated with any skull module (Supplementary Table S8), though they approached significance for the upper bill in the non-Malagasy vangas ( $p = 0.063$ ).

Modularity was consistently higher in the Malagasy than the non-Malagasy vangas; this result was highly significant for the upper and lower bills ( $p < 0.001$ ) but not for the

upper bill and neurocranium (Table 2). In both cases, removing *Falculea*, *Euryceros*, or both always decreased the degree of modularity in the remaining Malagasy dataset. Removing *Euryceros* or both outliers resulted in the remaining Malagasy vangas switching to showing significantly lower modularity than the non-Malagasy vangas, while removing *Falculea* alone had a more variable impact. Examining the distribution of null covariance ratios from the resampling procedure for each test suggested that wide variation in the mean and standard error of these distributions between datasets may explain at least some of the surprising variation in modularity and significance tests (Supplementary Figure

**Table 2.** Pairwise comparisons of the strength of skull modularity between Malagasy and non-Malagasy vangas.

	Malagasy	Non-Malagasy	Malagasy (no outliers)	Malagasy (no <i>Falculea</i> )	Malagasy (no <i>Euryceros</i> )
Upper bill vs. neurocranium					
$Z_{CR}$ (Modularity)	-15.523	-7.946	-6.047	-9.812	-5.280
Malagasy	-	0.057	<b>3.641</b>	<b>4.955</b>	<b>12.567</b>
Non-Malagasy	0.954	-	<b>2.696</b>	<b>3.139</b>	<b>6.778</b>
Malagasy (no outliers)	<0.001	0.007	-	0.084	<b>4.521</b>
Malagasy (no <i>Falculea</i> )	<0.001	0.002	0.933	-	<b>6.932</b>
Malagasy (no <i>Euryceros</i> )	<0.001	<0.001	<0.001	<0.001	-
Upper bill vs. lower bill					
$Z_{CR}$ (Modularity)	-16.221	-14.223	-10.718	-12.129	-14.109
Malagasy	-	7.600	<b>4.127</b>	<b>6.466</b>	<b>11.696</b>
Non-Malagasy	<0.001	-	<b>2.746</b>	0.208	<b>12.625</b>
Malagasy (no outliers)	<0.001	0.006	-	<b>2.336</b>	9.090
Malagasy (no <i>Falculea</i> )	<0.001	0.835	0.019	-	<b>10.751</b>
Malagasy (no <i>Euryceros</i> )	<0.001	<0.001	<0.001	<0.001	-

**Note.** Modularity is quantified as the covariance ratio (CR). ZCR is the strength of modularity for each clade, with a more negative Z score indicating greater modularity—the Malagasy vangas (with outliers included) are the most modular. Pairwise comparisons of modularity between clades (Malagasy, non-Malagasy, and Malagasy with outliers removed), with Z scores above and *p*-values below the diagonal. Significant differences are bolded.

[S5](#)). Overall, we did not find a consistent relationship between the morphological diversity of the Malagasy vangas and either integration or modularity; instead, we found that the results were broadly sensitive to the presence of anatomical outliers.

### Rates of trait evolution

For all traits except body size, our BayesTraits analyses found very strong evidence in support of more complex, rate-variable models over a constant rate of morphological evolution ([Supplementary Table S9](#)). The results for all three skull/bill datasets were essentially the same: We focus here on the full skull without post hoc rotation of outliers, but results from all three can be found in the Supplementary Material. The best-supported model for rates of vanga skull evolution was a reversible-jump branch transform where a scalar was applied to certain tips, indicating strong directional trends in shape in those taxa. Five branch scalars were found in greater than 85% of trees from the posterior, with consistent probabilities and magnitudes across five runs ([Figure 5](#), [Supplementary Table S10](#)). Shifts occurred in *Falculea* and *Euryceros* 100% of the time, with ~20–25-fold increases, while smaller shifts usually occurred in *Xenopirostris* and two members of the African genus *Prionops* ([Figure 5](#), [Supplementary Tables S10](#) and [S11](#)). The best-supported model for foot shape was a reversible-jump delta transform ([Supplementary Table S9](#)). This model found a delta transform of 1.76 at the root of all Vangidae in 100% of posterior trees, indicating a family-wide trend of accelerating foot evolution through time ([Supplementary Table S10](#)). An additional two delta transforms were detected in slightly under half of sampled trees: a second increase in delta of 1.18 at the ancestor of *Hypositta* plus the remaining Malagasy vangas, followed by a decrease in delta of 0.90 at the subsequent node (excluding *Hypositta*); this had the effect of a massive increase in evolutionary rate for *Hypositta* alone ([Supplementary Figure S6](#)). For body mass, we found moderate support for a node transform at the origin of the “derived” clade (Bayes factor = 2.78), indicating an increase in rates of size evolution in this group ([Supplementary Table S9](#)).

Our DTT results are largely congruent with our BayesTraits analyses, showing that average subclade dispar-

ity in skull shape does not conform to Brownian motion expectations in the Malagasy vangas ([Figure 5](#)). Subclade disparity stayed within BM expectations until a sharp increase about 12 Ma, at the common ancestor of *Euryceros* plus its sister taxa and the probing clade. It then stayed high and spiked about 4 Ma, just before *Falculea* and *Euryceros* split from their respective sister taxa, then declined sharply toward the present. Foot shape, in contrast, showed a steady decrease in disparity through time consistent with the null expectation of a Brownian model of morphological evolution ([Supplementary Figure S7](#)).

The net rate of multivariate trait evolution was 2–4× higher in the Malagasy vangas for each module except the neurocranium and for the whole skull, but removing the two outliers eliminated this difference ([Table 3](#)). The net evolutionary rate also differed significantly between vangas using different foraging behaviors ([Table 3](#)). The small but morphologically disparate probing clade consistently had the highest rates of skull evolution, up to 10.7× that of gleaners in the upper bill. However, the statistical significance of these differences varied by method. Rate differences were highly significant when tested using phylogenetic simulation ([Denton & Adams, 2015](#)), but not when using a permutation test ([Supplementary Table S12](#)) ([Adams & Collyer, 2018](#)). The difference between the two methods might be a consequence of permutation being more sensitive to the presence of outliers.

### Discussion

The Malagasy vangas constitute an adaptive radiation, with exceptional ecomorphological disparity associated with diversification of foraging mode. Taking the relatively uncommon approach of comparing the tempo and mode of evolution in a proposed radiation to that of its relatives ([Burress & Muñoz, 2022](#); [Starr et al., 2024](#)), we found higher disparity in the Malagasy vangas than in their relatives across all measured traits. This finding is consistent with a classic model of adaptive radiation in response to ecological opportunity, where the Malagasy vangas have diversified in traits that allow them to exploit a range of niches usually filled by other clades on the mainland ([Gillespie et al., 2020](#)). Much of this diversification was likely facilitated by

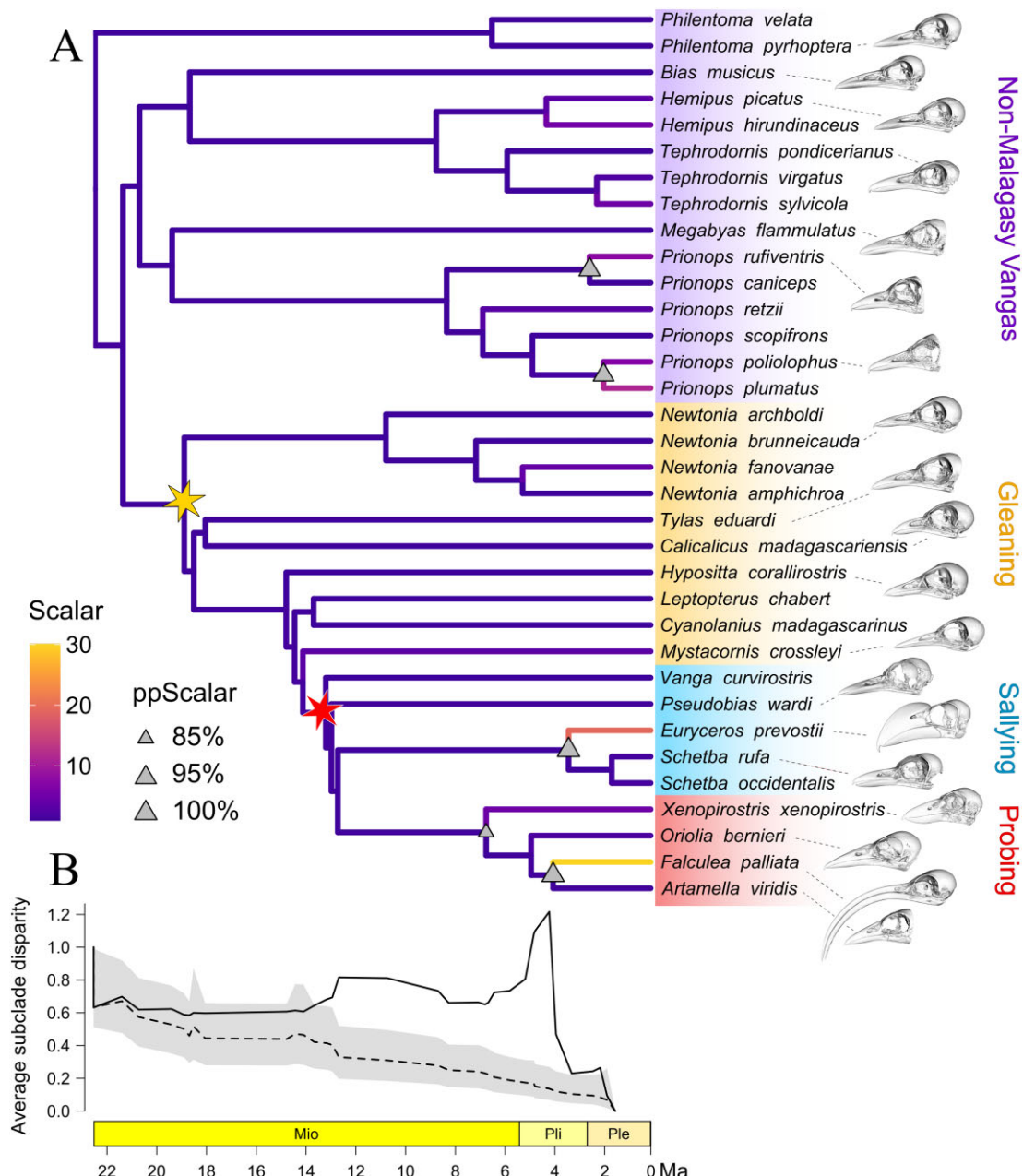


**Figure 5.** Rates of skull shape evolution in vangas. (A) Phylogeny of Vangidae with branches colored by magnitude of mean directional shifts in the best-supported model. This model suggests that large directional shifts in individual taxa have collectively generated the exceptional degree of morphological diversity observed in the Malagasy vangas. Triangles indicate shifts detected in over 85% of posterior trees, and stars indicate the colonization of Madagascar (yellow) and later the origin of the “derived” subclade (red). (B) Disparity through time plot, with solid line indicating observed disparity, dashed line simulated disparity under constant rates, and the shaded area the 95% confidence interval. Average subclade disparity was elevated through the diversification of the derived clade, peaking just before *Falculea* split from its sister species *Artamella*.

**Table 3.** Differences in the net rate of evolution for each anatomical region between clades (Malagasy vs. non-Malagasy vangas) and between foraging categories (probing, sallying, and gleaning).

Module	Malagasy vs. non-Mal	Probe vs. Glean	Probe vs. Sally	Glean vs. Sally
Whole skull	2.306 (0.001)	6.711 (0.001)	3.444 (0.001)	1.949 (0.001)
Skull (outliers excluded)	1.186 (0.160)	1.424 (0.0829)	1.881 (0.013)	1.321 (0.079)
Upper bill	4.034 (0.001)	10.893 (0.001)	2.953 (0.002)	3.689 (0.001)
Lower bill	2.760 (0.001)	8.759 (0.001)	6.349 (0.001)	1.380 (0.250)
Neurocranium	1.135 (0.462)	1.537 (0.108)	1.158 (0.618)	1.328 (0.166)
Feet	2.008 (0.003)	1.037 (0.919)	2.375 (0.024)	2.290 (0.002)
Feet (outliers excluded)	1.112 (0.630)	1.824 (0.056)	2.284 (0.021)	1.252 (0.373)

Note. Values are rate difference (fold) and *p*-values from the simulation procedure. Significant differences are bolded.

the evolution of new modes of foraging, as much of the novel bill shape variation in the Malagasy vangas is found in the subclade in which first sallying, and then probing types of foraging maneuvers evolved. However, these foraging categories do not account for the foraging substrates used by different species, which likely drive locomotor adaptations and therefore pedal shape variation. The most unique pedal morphologies are in gleaners with different locomotory demands: the terrestrial *Mystacornis* and *Hypositta*, a vertical climbing gleaner of trunks and branches. These traits have made generally independent contributions to vanga diversity: Different species display extreme morphologies in bill or foot shape, facilitating their specialization to an exceptionally wide range of foraging niches.

### Integration and modularity are heterogeneous within the Malagasy vangas

The results of our analyses of integration and modularity were complex, suggesting that the interaction between integration, modularity, and evolvability in vangas is not straightforward. When we excluded anatomical outliers, the Malagasy vangas generally had statistically indistinguishable levels of integration and significantly lower modularity than the non-Malagasy vangas, suggesting some role for reduced independence at least between skull modules in their diversification. However, the presence of a few species with highly divergent morphologies among the Malagasy vangas had profoundly affected our results. The impacts of excluding either of the two bill shape outliers alone or both together were highly variable, likely due to their very different morphologies. Although *Falculea* has by far the most unique bill shape among all vangas, standing out in every one of our analyses, that it remained an outlier in the PCA with post hoc rotation suggests an overall pattern of trait covariation partially reflecting that in the rest of Vangidae. *Euryceros*, in contrast, with its distinctive upper bill only, appears to show a unique pattern of trait covariation. Similarly, *Mystacornis* and *Hypositta* were not outliers in post hoc rotation plots of foot shape. *Euryceros* and *Falculea* were also outliers on different axes of the partial least-squares analysis plots, again suggesting contrasting modes of bill shape divergence.

Together, we take these results to suggest that the rapid evolution of *Falculea*'s extremely decurved bill may have required increasingly tight integration between the upper and lower mandibles, and occurred at least in part along existing evolutionary lines of least resistance (Felice et al., 2018; Schlüter, 1996). In *Euryceros*, the evolution of unusually decoupled mandibles required a break from the dominant pattern of covariation, as did the evolution of divergent foot morphologies. A previous study found higher levels of integration between the upper bill and neurocranium in the Galapagos finches and Hawaiian honeycreepers than in other passerine birds, but no general relationship between integration and rates of evolution (Navalón et al., 2020). They suggested that this relationship is likely to break down in older clades due to variation in selective pressures acting over many millions of years; our findings in vangas may reflect this, with relatively similar patterns of integration in most vangas that can be disrupted by strong divergent selection. Navalón et al. did not include the lower bill in their study, but it would be interesting to compare our results to other clades such as the Hawaiian honeycreepers, which also

include several taxa whose upper and lower bills appear unusually decoupled. Studies in younger radiations might also be better able to address whether shifting patterns of integration at genetic, developmental, and/or evolutionary levels may primarily contribute to the evolvability of certain clades (Jablonski, 2022; Klingenberg, 2008).

### Rapid morphological evolution, but no evidence for an early burst

Despite much higher net rates of evolution in the Malagasy than the non-Malagasy vangas for most ecomorphological traits, we did not find any evidence to support an early burst of morphological evolution coincident with the colonization of Madagascar. In the classic early burst model of adaptive radiation, declining ecological opportunity and therefore diversification rates through time mean disparity should partition between subclades early in the radiation's history, resulting in a rapid drop in relative subclade disparity (Harmon et al., 2003; Slater et al., 2010). Instead, subclade disparity for skull shape was initially within the null distribution, then increased and stayed well above BM expectations during the diversification of the most morphologically disparate sallying and probing vangas. These divergent taxa resulted in large but unevenly distributed recent increases in rates of bill shape diversification, with individual species diverging dramatically and in different directions rather than any general clade-wide pattern. In contrast, rates of foot shape evolution have generally increased through time across all vangas, with a single additional increase in *Hypositta*. Taken together, these results show that most of the morphological diversification of the Malagasy vangas occurred after they had already been present in Madagascar for millions of years and coincident with the evolution of novel foraging behaviors.

The delayed increase in bill shape diversification, concentrated in a clade in which derived foraging behaviors have evolved, is consistent with the model of a subclade-specific key innovation (Etienne & Haegeman, 2012; Slater & Pennell, 2014). These major categories of foraging behavior do not correspond directly with the diverse specific behaviors employed by vangas with specialized bill and foot shapes (e.g., probing in leaves vs. tree cavities) but could have functioned as general behavioral innovations that expanded the range of niche space available to the clade, permitting greater coexistence and therefore diversification (German et al., 2024). A range of extrinsic or intrinsic factors could have played a role in the timing of this shift. Extrinsic factors include shifts in climate or competitive dynamics with other clades. One possible intrinsic factor is limited genetic diversity due to small founder populations. Hybrid origins are increasingly recognized as common especially in young, rapid radiations (Gillespie et al., 2020; Marques et al., 2019; Martin & Richards, 2019; Seehausen, 2004; Wogan et al., 2023), and future work should test for the presence of reticulation events, which were recently shown to have contributed to species diversification in gembirds, another Malagasy radiation of similar age (DeBaun et al., 2023).

The niche of the founding population is another intrinsic factor frequently proposed to constrain adaptive radiation, with certain traits predisposing some lineages to diversify (Flohr et al., 2013; Jablonski, 2008; Miller et al., 2025; Ngoepe et al., 2023). In birds, granivory has been proposed

as a trait that facilitates diversification, largely because the two best-studied avian radiations, the Galapagos finches and Hawaiian honeycreepers, both evolved high dietary diversity from a granivorous ancestor (Lovette et al., 2002; Rundell & Price, 2009). Constraint imposed by insectivorous ancestry is therefore another possible explanation for the delay in bill shape diversification in Vangidae. Despite their diversity of foraging behaviors, vangas have not evolved the dietary diversity of other classic avian radiations. This restriction might be one explanation for the slower initial diversification rate in vangas. A different, though related explanation is that vangas may belong to a clade with lower baseline evolvability. Passerida, the large clade in which the finches and honeycreepers are both nested, shows exceptionally high rates of both morphological evolution and speciation (Felice & Goswami, 2018; Imfeld & Barker, 2022; Lovette et al., 2002; Oliveros et al., 2019; Vinciguerra & Burns, 2021), indicating a high propensity for diversification. In contrast, the vangas are in Corvidae, which show an increase in speciation rate at their base (Oliveros et al., 2019) but no corresponding overall increase in rates of skull shape evolution (Felice & Goswami, 2018).

Given the extremely divergent morphologies of the “derived” clade of Malagasy vangas, we think it highly unlikely that intraspecific variation or measurement error impacted our overall conclusions. We did detect the greatest rate shifts at the tips, but these were specifically in our most obviously anatomically extreme taxa, and fit into a broader pattern of increased disparity throughout the derived clade defined by foraging mode, and increased net evolutionary rates in these foraging categories. Also supporting this view, the next-highest supported model following the more complex reversible-jump models was one indicating a single rate shift at the origin of the derived clade (Supplementary Table S9).

### Outliers or extreme forms

The Malagasy vangas offer a very different model of adaptive radiation from that of the classic early burst, where instead many individual taxa have diverged dramatically in one or more aspects of their morphology to generate most of the disparity across the group. This presents substantial challenges to the quantitative analysis of trait diversity and evolution, as existing conceptual frameworks and empirical tests for understanding adaptive radiation are not well designed for groups in which divergent and extreme forms are essential to understanding the clade as a whole. This is not a new challenge. For example, Slater et al. (2010) did detect an early burst of morphological evolution in cetaceans, but only after removing young outliers, whereas Rowsey et al. (2019) lost support for an early burst in Philippine rodents when outliers were removed. Our confidence in the results of several analyses was complicated due to both the small number of taxa in Vangidae and the large impact of these outliers. This challenge may be inherent to our statistical approaches, but nonetheless needs to be accounted for in our biological interpretations.

### Conclusions and future directions

Vangas offer an example of an adaptive radiation that has achieved exceptional ecomorphological diversity, but not through an early burst of trait evolution. Our study demon-

strated the importance of using multiple traits to examine the complexities of morphological diversification in clades that are likely responding to varied selective pressures. We emphasized the importance of exceptional ecomorphological diversity as the unifying feature of adaptive radiations, and explored the impact of extreme phenotypes in driving diversification patterns. Our conclusions about integration and modularity were highly influenced by inclusion or removal of extreme taxa, indicating that there are idiosyncratic patterns of trait covariation in anatomically disparate vangas. These results suggest that integration patterns may be generally conserved but can also evolve relatively rapidly in specific traits under divergent selective pressures. The evolution of novel classes of foraging behavior can be considered a “key innovation” in Malagasy vangas, but this alone does not explain the higher phenotypic diversity in this clade, as other related factors such as locomotory mode have driven diversification in different directions.

In this study, we took a sister clade approach to evaluating the diversification of Malagasy vangas. However, a more complete understanding of biodiversity patterns and their causes will require broadening taxonomic scope to comparisons across a wider range of taxa, without losing the insights that emerge from species-level sampling (Losos & Miles, 2002; Moen et al., 2021). We highlight the importance of future studies to explore the frequency of outliers, i.e., species exhibiting extremely divergent morphologies, across traits and taxonomic scales, and to investigate whether this is a more general feature of many adaptive radiations, as some other authors have suggested (Martin & Richards, 2019; Rowsey et al., 2020; Slater & Pennell, 2014). A survey of this phenomenon would help evaluate how extreme phenotypes should fit into our conceptual frameworks and be accounted for in analyses of macroevolution.

### Supplementary material

Supplementary material is available online at *Evolution*.

### Data availability

All data and scripts associated with this study are available through the Dryad digital data repository (doi: 10.5061/dryad.ttdz08m8q). New CT scans generated as part of this study have been added to the MorphoSource repository (morphosource.org).

### Author contributions

A.A. and S.R. designed research; A.A., E.L., and S.R. performed research and analyzed data; and A.A. and S.R. wrote the paper with contributions from all authors.

### Funding

This work was supported by the National Science Foundation DEB-1457624 and DEB-2321548 awarded to S.R.; Dayton and Simons Foundation Canada Fellowships and a Davenport Award from the Bell Museum to A.A.; a Huempfner Award from University of Minnesota Department of Ecology, Evolution and Behavior to A.A.; and an award from the UMN Office of Undergraduate Research to E.L.

## Conflict of interest

The authors declare no conflicting interests.

## Acknowledgments

We gratefully acknowledge the collections staff for use of specimens sampled for this study, including Ben Marks, John Bates, and Shannon Hackett at the Field Museum and Paul Sweet and Thomas Trombone at the American Museum of Natural History. We thank Kelsi Hurdle and Aki Watanabe (NYIT Visualization Center, funded by NSF 1828305), David Birlenbach, Gabriele Ilarde, and Francesca Socki (UMN XRCT Lab), April Neander and Zhe-Xi Luo (University of Chicago PaleoCT), and Thom Sanger and Jim Cheverud (Loyola University Chicago) for CT scanning access and assistance. Abby Brett and Anna Flucke helped process CT scans. Access to scans on MorphoSource was provided by Roger Benson, and by the Field Museum of Natural History and the Yale Peabody Museum with funding from the oVert project (NSF DBI-1701714). We thank Keith Barker, Shanta Hejmadi, Tyler Imfeld, Sharon Jansa, Kieran McNulty, Hélène Morlon, Emma Sherratt, and one anonymous reviewer for their feedback on earlier versions of this manuscript and the entire Reddy–Barker–Jansa–Ford lab group for helpful discussions and support.

## References

3D Slicer. 2020. 3D Slicer image computing platform. <https://slicer.org/>. Date accessed December 5, 2023.

Abourachid, A., Fabre, A.-C., Cornette, R., & Höfling, E. (2017). Foot shape in arboreal birds: Two morphological patterns for the same pincer-like tool. *Journal of Anatomy*, 231, 1–11. <https://doi.org/10.1111/joa.12614>

Ackerly, D.D., Schwilk, D.W., & Webb, C.O. (2006). Niche evolution and adaptive radiation: Testing the order of trait divergence. *Ecology*, 87, S50–S61. [https://doi.org/10.1890/0012-9658\(2006\)75b:S50:NEAART%5d2.0.CO;2](https://doi.org/10.1890/0012-9658(2006)75b:S50:NEAART%5d2.0.CO;2)

Adams, D., Collyer, M., Kaliontzopoulou, A., & Baken, E. (2024). geomorph: Geometric morphometric analyses of 2D and 3D landmark data. [CRAN.R-project.org/package=geomorph](https://CRAN.R-project.org/package=geomorph). Date accessed March 5, 2024.

Adams, D.C. (2014a). A method for assessing phylogenetic least squares models for shape and other high-dimensional multivariate data. *Evolution*, 68, 2675–2688. <https://doi.org/10.1111/evo.12463>

Adams, D.C. (2014b). Quantifying and comparing phylogenetic evolutionary rates for shape and other high-dimensional phenotypic data. *Systematic Biology*, 63, 166–177. <https://doi.org/10.1093/sysbio/syt105>

Adams, D.C. (2016). Evaluating modularity in morphometric data: Challenges with the RV coefficient and a new test measure. *Methods in Ecology and Evolution*, 7, 565–572. <https://doi.org/10.1111/2041-210X.12511>

Adams, D.C., & Collyer, M.L. (2016). On the comparison of the strength of morphological integration across morphometric datasets. *Evolution*, 70, 2623–2631. <https://doi.org/10.1111/evo.13045>

Adams, D.C., & Collyer, M.L. (2018). Multivariate phylogenetic comparative methods: Evaluations, comparisons, and recommendations. *Systematic Biology*, 67, 14–31. <https://doi.org/10.1093/sysbio/syx055>

Adams, D.C., & Collyer, M.L. (2019). Comparing the strength of modular signal, and evaluating alternative modular hypotheses, using covariance ratio effect sizes with morphometric data. *Evolution*, 73, 2352–2367. <https://doi.org/10.1111/evo.13867>

Adams, D.C., & Felice, R.N. (2014). Assessing trait covariation and morphological integration on phylogenies using evolutionary covariance matrices. *PLoS One*, 9, e94335. <https://doi.org/10.1371/journal.pone.0094335>

Astudillo-Clavijo, V., Arbour, J.H., & López-Fernández, H. (2015). Selection towards different adaptive optima drove the early diversification of locomotor phenotypes in the radiation of neotropical geophagine cichlids. *BMC Evolutionary Biology*, 15, 77. <https://doi.org/10.1186/s12862-015-0348-7>

Autodesk Inc. (2018). Autodesk Meshmixer. [meshmixer.com](http://meshmixer.com). Date accessed June 7, 2024.

Baken, E.K., Collyer, M.L., Kaliontzopoulou, A., & Adams, D.C. (2021). geomorph v4.0 and gmShiny: Enhanced analytics and a new graphical interface for a comprehensive morphometric experience. *Methods in Ecology and Evolution*, 12, 2355–2363. <https://doi.org/10.1111/2041-210X.13723>

Barreto, E., Lim, M.C.W., Rojas, D., Dávalos, L.M., Wüest, R.O., Machac, A., & Graham, C.H. (2023). Morphology and niche evolution influence hummingbird speciation rates. *Proceedings of the Royal Society B: Biological Sciences*, 290, 20221793. <https://doi.org/10.1098/rspb.2022.1793>

Blonder, B. (2016). Do hypervolumes have holes? *The American Naturalist*, 187, E93–E105. <https://doi.org/10.1086/685444>

Blonder, B., Morrow, C.B., Maitner, B., Harris, D.J., Lamanna, C., Vilolle, C., Enquist, B.J., & Kerkhoff, A.J. (2018). New approaches for delineating  $n$ -dimensional hypervolumes. *Methods in Ecology and Evolution*, 9, 305–319. <https://doi.org/10.1111/2041-210X.12865>

Bookstein, F.L. (1997). Landmark methods for forms without landmarks: Morphometrics of group differences in outline shape. *Medical Image Analysis*, 1, 225–243. [https://doi.org/10.1016/S1361-8415\(97\)85012-8](https://doi.org/10.1016/S1361-8415(97)85012-8)

Bookstein, F.L., Gunz, P., Mitteroecker, P., Prossinger, H., Schäfer, K., & Seidler, H. (2003). Cranial integration in homo: Singular warps analysis of the midsagittal plane in ontogeny and evolution. *Journal of Human Evolution*, 44, 167–187. [https://doi.org/10.1016/S0047-2484\(02\)00201-4](https://doi.org/10.1016/S0047-2484(02)00201-4)

Bouckaert, R., Vaughan, T.G., Barido-Sottani, J., Duchêne, S., Fourment, M., Gavryushkina, A., Heled, J., Jones, G., Kühnert, D., Maio, N.D., Matschiner, M., Mendes, F.K., Müller, N.F., Ogilvie, H.A., du Plessis, L., Popinga, A., Rambaut, A., Rasmussen, D., Siveroni, I., ... Drummond, A.J. (2019). BEAST 2.5: An advanced software platform for Bayesian evolutionary analysis. *PLOS Computational Biology*, 15, e1006650. <https://doi.org/10.1371/journal.pcbi.1006650>

Burress, E.D., & Muñoz, M.M. (2021). Ecological opportunity from innovation, not islands, drove the anole lizard adaptive radiation. *Systematic Biology*, 71, 93–104. <https://doi.org/10.1093/sysbio/syab031>

Cardini, A. (2017). Left, right or both? Estimating and improving accuracy of one-side-only geometric morphometric analyses of cranial variation. *Journal of Zoological Systematics and Evolutionary Research*, 55, 1–10. <https://doi.org/10.1111/jzs.12144>

Cardini, A. (2019). Integration and modularity in procrustes shape data: Is there a risk of spurious results? *Evolutionary Biology*, 46, 90–105. <https://doi.org/10.1007/s11692-018-9463-x>

Cardini, A., & Marco, V.A. (2022). Procrustes shape cannot be analyzed, interpreted or visualized one landmark at a time. *Evolutionary Biology*, 49, 239–254. <https://doi.org/10.1007/s11692-022-09565-1>

Chen, D., Hosner, P.A., Dittmann, D.L., O'Neill, J.P., Birks, S.M., Braun, E.L., & Kimball, R.T. (2021). Divergence time estimation of Galliformes based on the best gene shopping scheme of ultra-conserved elements. *BMC Ecology and Evolution*, 21, 209. <https://doi.org/10.1186/s12862-021-01935-1>

Cheverud, J.M. (1984). Quantitative genetics and developmental constraints on evolution by selection. *Journal of Theoretical Biology*, 110, 155–171. [https://doi.org/10.1016/S0022-5193\(84\)80050-8](https://doi.org/10.1016/S0022-5193(84)80050-8)

**Chhaya, V.**, Reddy, S., & Krishnan, A. (2023). Bill shape imposes biomechanical tradeoffs in cavity-excavating birds. *Proceedings of the Royal Society B: Biological Sciences*, 290, 20222395. <https://doi.org/10.1098/rspb.2022.2395>

**Claramunt, S.**, & Cracraft, J. (2015). A new time tree reveals Earth history's imprint on the evolution of modern birds. *Science Advances*, 1, e1501005.

**Clavel, J.**, & Morlon, H. (2020). Reliable phylogenetic regressions for multivariate comparative data: Illustration with the MANOVA and application to the effect of diet on mandible morphology in phyllostomid bats. *Systematic Biology*, 69, 927–943. <https://doi.org/10.1093/sysbio/syaa010>

**Clavel, J.**, Aristide, L., & Morlon, H. (2019). A penalized likelihood framework for high-dimensional phylogenetic comparative methods and an application to new-world monkeys brain evolution. *Systematic Biology*, 68, 93–116.

**Clements, J.F.**, Rasmussen, P.C., Schulenberg, T.S., Iliff, M.J., Fredericks, T.A., Gerbracht, J.A., Lepage, D., Spencer, A., Billerman, S.M., Sullivan, B.L., & Wood, C.L. (2023). The eBird/Clements Checklist of Birds of the World: v2023. Downloaded from [www.birds.cornell.edu/clementschecklist/download/](http://www.birds.cornell.edu/clementschecklist/download/). Date accessed March 7, 2024.

**Collyer, M.**, & Adams, D. (2024). RRPP: Linear model evaluation with randomized residuals in a permutation procedure. [CRAN.R-project.org/package=RRPP](https://CRAN.R-project.org/package=RRPP). Date accessed March 26, 2024.

**Collyer, M.L.**, & Adams, D.C. (2018). RRPP: An R package for fitting linear models to high-dimensional data using residual randomization. *Methods in Ecology and Evolution*, 9, 1772–1779. <https://doi.org/10.1111/2041-210X.13029>

**Collyer, M.L.**, Baken, E.K., & Adams, D.C. (2022). A standardized effect size for evaluating and comparing the strength of phylogenetic signal. *Methods in Ecology and Evolution*, 13, 367–382. <https://doi.org/10.1111/2041-210X.13749>

**Conaway, M.A.**, & Adams, D.C. (2022). An effect size for comparing the strength of morphological integration across studies. *Evolution*, 76, 2244–2259. <https://doi.org/10.1111/evo.14595>

**Conith, A.J.**, Hope, S.A., Chhouk, B.H., & Craig Albertson, R. (2021). Weak genetic signal for phenotypic integration implicates developmental processes as major regulators of trait covariation. *Molecular Ecology*, 30, 464–480. <https://doi.org/10.1111/mec.15748>

**Cooney, C.R.**, & Thomas, G.H. (2021). Heterogeneous relationships between rates of speciation and body size evolution across vertebrate clades. *Nature Ecology & Evolution*, 5, 101–110. <https://doi.org/10.1038/s41559-020-01321-y>

**Cooney, C.R.**, Bright, J.A., Capp, E.J.R., Chira, A.M., Hughes, E.C., Moody, C.J.A., Nouri, L.O., Varley, Z.K., & Thomas, G.H. (2017). Mega-evolutionary dynamics of the adaptive radiation of birds. *Nature*, 542, 344–347. <https://doi.org/10.1038/nature21074>

**Cooper, N.**, Thomas, G.H., Venditti, C., Meade, A., & Freckleton, R.P. (2016). A cautionary note on the use of Ornstein Uhlenbeck models in macroevolutionary studies. *Biological Journal of the Linnean Society*, 118, 64–77. <https://doi.org/10.1111/bij.12701>

**De-Kayne, R.**, Schley, R., Barth, J.M.I., Campillo, L.C., Chaparro-Pedraza, C., Joshi, J., Salzburger, W., Bocxlaer, B.V., Cotoras, D.D., Fruciano, C., Geneva, A.J., Gillespie, R., Heras, J., Koblmüller, S., Matthews, B., Onstein, R.E., Seehausen, O., Singh, P., Svensson, E.I., & Cercá, J. (2024). Why do some lineages radiate while others do not? Perspectives for future research on adaptive radiations. *Cold Spring Harbor Perspectives in Biology*, 17, a041448.

**DeBaun, D.**, Rabibisoa, N., Raselimanana, A.P., Raxworthy, C.J., & Burbink, F.T. (2023). Widespread reticulate evolution in an adaptive radiation. *Evolution*, 77, 931–945. <https://doi.org/10.1093/evolut/qpad011>

**Dehling, D.M.**, Jordano, P., Schaefer, H.M., Böhning-Gaese, K., & Schleuning, M. (2016). Morphology predicts species' functional roles and their degree of specialization in plant-frugivore interactions. *Proceedings of the Royal Society B: Biological Sciences*, 283, 20152444. <https://doi.org/10.1098/rspb.2015.2444>

**Dellinger, A.S.**, Artuso, S., Pamperl, S., Michelangeli, F.A., Penneys, D.S., Fernández-Fernández, D.M., Alvear, M., Almeda, F., Scott Armbruster, W., Staedler, Y., & Schönenberger, J. (2019). Modularity increases rate of floral evolution and adaptive success for functionally specialized pollination systems. *Communications Biology*, 2, 1–11.

**Denton, J.S.S.**, & Adams, D.C. (2015). A new phylogenetic test for comparing multiple high-dimensional evolutionary rates suggests interplay of evolutionary rates and modularity in lanternfishes (Mycophiformes: Myctophidae). *Evolution*, 69, 2425–2440. <https://doi.org/10.1111/evo.12743>

**Derryberry, E.P.**, Claramunt, S., Derryberry, G., Chesser, R.T., Cracraft, J., Aleixo, A., Pérez-Emán, J., Remsen, J.V., & Brumfield, R.T. (2011). Lineage diversification and morphological evolution in a large-scale continental radiation: The neotropical ovenbirds and woodcreepers (Aves: Furnariidae). *Evolution*, 65, 2973–2986. <https://doi.org/10.1111/j.1558-5646.2011.01374.x>

**Dickinson, E.**, Young, M.W., Flaim, N.D., Sawiec, A., & Granatosky, M.C. (2023). A functional framework for interpreting phalangeal form. *Journal of the Royal Society Interface*, 20, 20230251. <https://doi.org/10.1098/rsif.2023.0251>

**Donoghue, M.J.**, & Sanderson, M.J. (2015). Confluence, synnovation, and depauperons in plant diversification. *New Phytologist*, 207, 260–274. <https://doi.org/10.1111/nph.13367>

**Eliason, C.M.**, McCullough, J.M., Andersen, M.J., & Hackett, S.J. (2021). Accelerated brain shape evolution is associated with rapid diversification in an avian radiation. *The American Naturalist*, 197, 576–591. <https://doi.org/10.1086/713664>

**Eliason, C.M.**, Straker, L., Jung, S., & Hackett, S.J. (2020). Morphological innovation and biomechanical diversity in plunge-diving birds. *Evolution*, 74, 1514–1524. <https://doi.org/10.1111/evo.14024>

**Etienne, R.S.**, & Haegeman, B. (2012). A conceptual and statistical framework for adaptive radiations with a key role for diversity dependence. *The American Naturalist*, 180, E75–E89. <https://doi.org/10.1086/667574>

**Evans, K.M.**, Larouche, O., Watson, S.-J., Farina, S., Habegger, M.L., & Friedman, M. (2021). Integration drives rapid phenotypic evolution in flatfishes. *Proceedings of the National Academy of Sciences*, 118, e2101330118. <https://doi.org/10.1073/pnas.2101330118>

**Falk, A.R.**, Lamsdell, J.C., & Gong, E. (2021). Principal component analysis of avian hind limb and foot morphometrics and the relationship between ecology and phylogeny. *Paleobiology*, 47, 314–336. <https://doi.org/10.1017/pab.2020.39>

**Fedorov, A.**, Beichel, R., Kalpathy-Cramer, J., Finet, J., Fillion-Robin, J.-C., Pujol, S., Bauer, C., Jennings, D., Fennessy, F., Sonka, M., Buatti, J., Aylward, S., Miller, J.V., Pieper, S., & Kikinis, R. (2012). 3D Slicer as an image computing platform for the Quantitative Imaging Network. *Magnetic Resonance Imaging*, 30, 1323–1341. <https://doi.org/10.1016/j.mri.2012.05.001>

**Felice, R.N.**, & Goswami, A. (2018). Developmental origins of mosaic evolution in the avian cranium. *Proceedings of the National Academy of Sciences*, 115, 555–560. <https://doi.org/10.1073/pnas.1716437115>

**Felice, R.N.**, Randau, M., & Goswami, A. (2018). A fly in a tube: Macroevolutionary expectations for integrated phenotypes. *Evolution*, 72, 2580–2594. <https://doi.org/10.1111/evo.13608>

**Flohr, R.C.E.**, Blom, C.J., Rainey, P.B., & Beaumont, H.J.E. (2013). Founder niche constrains evolutionary adaptive radiation. *Proceedings of the National Academy of Sciences*, 110, 20663–20668. <https://doi.org/10.1073/pnas.1310310110>

**Folk, R.A.**, Stubbs, R.L., Mort, M.E., Cellinese, N., Allen, J.M., Soltis, P.S., Soltis, D.E., & Guralnick, R.P. (2019). Rates of niche and phenotype evolution lag behind diversification in a temperate radiation. *Proceedings of the National Academy of Sciences*, 116, 10874–10882. <https://doi.org/10.1073/pnas.1817999116>

**Freckleton, R.P.**, & Harvey, P.H. (2006). Detecting non-Brownian trait evolution in adaptive radiations. *PLoS Biology*, 4, e373. <https://doi.org/10.1371/journal.pbio.0040373>

**Gavrilets, S.**, & Losos, J.B. (2009). Adaptive radiation: Contrasting theory with data. *Science*, 323, 732–737. <https://doi.org/10.1126/science.1157966>

**Germain, R.M.**, Matthews, B., & Harmon, L. (2024). Niche theory as an underutilized resource for the study of adaptive radiations. *Cold Spring Harbor Perspectives in Biology*, 17, a041449.

**Gillespie, R.G.**, Bennett, G.M., De Meester, L., Feder, J.L., Fleischer, R.C., Harmon, L.J., Hendry, A.P., Knope, M.L., Mallet, J., Martin, C., Parent, C.E., Patton, A.H., Pfennig, K.S., Rubinoff, D., Schlüter, D., Seehausen, O., Shaw, K.L., Stacy, E., Stervander, M., & Wogan, G.O.U. (2020). Comparing adaptive radiations across space time, and taxa. *Journal of Heredity*, 111, 1–20. <https://doi.org/10.1093/jhered/esz064>

**Givnish, T.J.** (2015). Adaptive radiation versus “radiation” and “explosive diversification”: Why conceptual distinctions are fundamental to understanding evolution. *New Phytologist*, 207, 297–303. <https://doi.org/10.1111/nph.13482>

**Givnish, T.J.**, & Sytsma, K.J. (1997). *Molecular evolution and adaptive radiation*. Cambridge University Press.

**Glor, R.E.** (2010). Phylogenetic insights on adaptive radiation. *Annual Review of Ecology, Evolution, and Systematics*, 41, 251–270. <https://doi.org/10.1146/annurev.ecolsys.39.110707.173447>

**Goswami, A.**, Smaers, J.B., Soligo, C., & Polly, P.D. (2014). The macroevolutionary consequences of phenotypic integration: From development to deep time. *Philosophical Transactions of the Royal Society B: Biological Sciences*, 369, 20130254. <https://doi.org/10.1098/rstb.2013.0254>

**Gower, J.C.** (1975). Generalized Procrustes analysis. *Psychometrika*, 40, 33–51. <https://doi.org/10.1007/BF02291478>

**Griswold, C.K.** (2006). Pleiotropic mutation, modularity and evolvability. *Evolution & Development*, 8, 81–93. <https://doi.org/10.1111/j.1525-142X.2006.05077.x>

**Grossnickle, D.M.**, Sadier, A., Patterson, E., Cortés-Viruet, N.N., Jiménez-Rivera, S.M., Sears, K.E., & Santana, S.E. (2024). The hierarchical radiation of phyllostomid bats as revealed by adaptive molar morphology. *Current Biology*, 34, 1284–1294.e3. <https://doi.org/10.1016/j.cub.2024.02.027>

**Guillerme, T.**, Cooper, N., Brusatte, S.L., Davis, K.E., Jackson, A.L., Gerber, S., Goswami, A., Healy, K., Hopkins, M.J., Jones, M.E.H., Lloyd, G.T., O'Reilly, J.E., Pate, A., Puttick, M.N., Rayfield, E.J., Saupe, E.E., Sherratt, E., Slater, G.J., Weisbecker, V., & Donoghue, P.C.J. (2020). Disparities in the analysis of morphological disparity. *Biology Letters*, 16, 20200199. <https://doi.org/10.1098/rsbl.2020.0199>

**Harmon, L.J.**, Losos, J.B., Jonathan Davies, T., Gillespie, R.G., Gittemeier, J.L., Bryan Jennings, W., Kozak, K.H., McPeek, M.A., Moreno-Roark, F., Near, T.J., Purvis, A., Ricklefs, R.E., Schlüter, D., Schulte, J.A., Seehausen, O., Sidlauskas, B.L., Torres-Carvajal, O., Weir, J.T., & Ø. Mooers, A. (2010). Early bursts of body size and shape evolution are rare in comparative data. *Evolution*, 64, 2385–2396. .

**Harmon, L.J.**, Schulte, J.A., Larson, A., & Losos, J.B. (2003). Tempo and mode of evolutionary radiation in Iguanian lizards. *Science*, 301, 961–964. <https://doi.org/10.1126/science.1084786>

**Hedrick, B.P.**, Mutumi, G.L., Munteanu, V.D., Sadier, A., Davies, K.T.J., Rossiter, S.J., Sears, K.E., Dávalos, L.M., & Dumont, E. (2020). Morphological diversification under high integration in a hyper diverse mammal clade. *Journal of Mammalian Evolution*, 27, 563–575. <https://doi.org/10.1007/s10914-019-09472-x>

**Hodges, S.A.**, & Dierieg, N.J. (2009). Adaptive radiations: From field to genomic studies. *Proceedings of the National Academy of Sciences*, 106, 9947–9954.

**Imfeld, T.S.**, & Barker, F.K. (2022). Songbirds of the Americas show uniform morphological evolution despite heterogeneous diversification. *Journal of Evolutionary Biology*, 35, 1335–1351. <https://doi.org/10.1111/jeb.14084>

**Jablonski, D.** (2008). Species selection: Theory and data. *Annual Review of Ecology, Evolution, and Systematics*, 39, 501–524. <https://doi.org/10.1146/annurev.ecolsys.39.110707.173510>

**Jablonski, D.** (2022). Evolvability and macroevolution: Overview and synthesis. *Evolutionary Biology*, 49, 265–291. <https://doi.org/10.1007/s11692-022-09570-4>

**Johansson, U.S.**, Bowie, R.C.K., Hackett, S.J., & Schulenberg, T.S. (2008). The phylogenetic affinities of Crossley's babbler (*Mystacornis crossleyi*): Adding a new niche to the vanga radiation of Madagascar. *Biology Letters*, 4, 677–680. <https://doi.org/10.1098/rsbl.2008.0444>

**Jønsson, K.A.**, Fabre, P.-H., Fritz, S.A., Etienne, R.S., Ricklefs, R.E., Jørgensen, T.B., Fjeldså, J., Rahbek, C., Ericson, P.G.P., Woog, F., Pasquet, E., & Irestedt, M. (2012). Ecological and evolutionary determinants for the adaptive radiation of the Madagascan vangas. *Proceedings of the National Academy of Sciences*, 109, 6620–6625. <https://doi.org/10.1073/pnas.1115835109>

**Kassen, R.** (2009). Toward a general theory of adaptive radiation. *Annals of the New York Academy of Sciences*, 1168, 3–22. <https://doi.org/10.1111/j.1749-6632.2009.04574.x>

**Kirschner, M.**, & Gerhart, J. (1998). Evolvability. *Proceedings of the National Academy of Sciences*, 95, 8420–8427. <https://doi.org/10.1073/pnas.95.15.8420>

**Klingenberg, C.P.** (2008). Morphological integration and developmental modularity. *Annual Review of Ecology, Evolution, and Systematics*, 39, 115–132. <https://doi.org/10.1146/annurev.ecolsys.37.091305.110054>

**Krishnan, A.** (2023). Biomechanics illuminates form–function relationships in bird bills. *Journal of Experimental Biology*, 226, jeb245171. <https://doi.org/10.1242/jeb.245171>

**Lanfear, R.**, Frandsen, P.B., Wright, A.M., Senfeld, T., & Calcott, B. (2017). PartitionFinder 2: New methods for selecting partitioned models of evolution for molecular and morphological phylogenetic analyses. *Molecular Biology and Evolution*, 34, 772–773. .

**Larouche, O.**, Zelditch, M.L., & Cloutier, R. (2018). Modularity promotes morphological divergence in ray-finned fishes. *Scientific Reports*, 8, 7278. <https://doi.org/10.1038/s41598-018-25715-y>

**Losos, J.B.** (2010). Adaptive radiation, ecological opportunity, and evolutionary determinism. *The American Naturalist*, 175, 623–639. <https://doi.org/10.1086/652433>

**Losos, J.B.**, & Mahler, D.L. (2010). Adaptive radiation: The interaction of ecological opportunity, adaptation, and speciation. In M. A. Bell, D. J. Futuyma, W. F. Eanes, & J. S. Levinton (Eds.), *Evolution after Darwin: The first 150 years*(pp. 381–420). Sinauer Press.

**Losos, J.B.**, & Miles, D.B. (2002). Testing the hypothesis that a clade has adaptively radiated: Iguanid lizard clades as a case study. *The American Naturalist*, 160, 147–157. <https://doi.org/10.1086/341557>

**Lovette, I.J.**, Birmingham, E., & Ricklefs, R.E. (2002). Clade-specific morphological diversification and adaptive radiation in Hawaiian songbirds. *Proceedings of the Royal Society of London. Series B: Biological Sciences*, 269, 37–42. <https://doi.org/10.1098/rspb.2001.1789>

**Lucas, T.**, & Goswami, A. (2017). paleomorph: Geometric morphometric tools for paleobiology. [CRAN.R-project.org/package=paleomorph](https://CRAN.R-project.org/package=paleomorph). Date accessed April 3, 2024.

**Mahler, D.L.**, Revell, L.J., Glor, R.E., & Losos, J.B. (2010). Ecological opportunity and the rate of morphological evolution in the diversification of greater antillean anoles. *Evolution*, 64, 2731–2745. <https://doi.org/10.1111/j.1558-5646.2010.01026.x>

**Marques, D.A.**, Meier, J.I., & Seehausen, O. (2019). A combinatorial view on speciation and adaptive radiation. *Trends in Ecology & Evolution*, 34, 531–544. <https://doi.org/10.1016/j.tree.2019.02.008>

**Martin, B.S.**, Bradburd, G.S., Harmon, L.J., & Weber, M.G. (2023). Modeling the evolution of rates of continuous trait evolution. *Systematic Biology*, 72, 590–605. <https://doi.org/10.1093/sysbio/syac068>

**Martin, C.H.**, & Richards, E.J. (2019). The paradox behind the pattern of rapid adaptive radiation: How can the speciation process sustain itself through an early burst? *Annual Review of Ecology, Evolution, and Systematics*, 50, 569–593. <https://doi.org/10.1146/annurev-ecolsys-110617-062443>

Miles, D.B., & Ricklefs, R.E. (1984). The correlation between ecology and morphology in deciduous forest passerine birds. *Ecology*, 65, 1629–1640. <https://doi.org/10.2307/1939141>

Miller, E.C., Faucher, R., Hart, P.B., Rincón-Sandoval, M., Santaquiteria, A., White, W.T., Baldwin, C.C., Miya, M., Betancur-R, R., Tornabene, L., Evans, K., & Arcila, D. (2025). Reduced evolutionary constraint accompanies ongoing radiation in deep-sea anglerfishes. *Nature Ecology & Evolution*, 9, 474–490.

Moen, D.S., Ravelojaona, R.N., Hutter, C.R., & Wiens, J.J. (2021). Testing for adaptive radiation: A new approach applied to Madagascar frogs. *Evolution*, 75, 3008–3025. <https://doi.org/10.1111/evo.14328>

Mosleh, S., Choi, G.P.T., Musser, G.M., James, H.F., Abzhanov, A., & Mahadevan, L. (2023). Beak morphometry and morphogenesis across avian radiations. *Proceedings of the Royal Society B: Biological Sciences*, 290, 20230420. <https://doi.org/10.1098/rspb.2023.0420>

Mutumi, G.L., Hall, R.P., Hedrick, B.P., Yohe, L.R., Sadier, A., Davies, K.T.J., Rossiter, S.J., Sears, K.E., Dávalos, L.M., & Dumont, E.R. (2023). Disentangling mechanical and sensory modules in the radiation of noctilionoid bats. *The American Naturalist*, 202, 216–230. <https://doi.org/10.1086/725368>

Navalón, G., Marugán-Lobón, J., Bright, J.A., Cooney, C.R., & Rayfield, E.J. (2020). The consequences of craniofacial integration for the adaptive radiations of Darwin's finches and Hawaiian honeycreepers. *Nature Ecology & Evolution*, 4, 270–278. <https://doi.org/10.1038/s41559-019-1092-y>

Ngoepe, N., Muschick, M., Kishe, M.A., Mwaiko, S., Temoltzin-Loranca, Y., King, L., Courtney Mustaphi, C., Heiri, O., Wienhues, G., Vogel, H., Cuenca-Cambronero, M., Tinner, W., Grosjean, M., Matthews, B., & Seehausen, O. (2023). A continuous fish fossil record reveals key insights into adaptive radiation. *Nature*, 622, 315–320. <https://doi.org/10.1038/s41586-023-06603-6>

Oliveros, C.H., Field, D.J., Ksepka, D.T., Barker, F.K., Aleixo, A., Andersen, M.J., Alström, P., Benz, B.W., Braun, E.L., Braun, M.J., Bravo, G.A., Brumfield, R.T., Chesser, R.T., Claramunt, S., Cracraft, J., Cuervo, A.M., Derryberry, E.P., Glenn, T.C., Harvey, M.G., & Faircloth, B.C. (2019). Earth history and the passerine superradiation. *Proceedings of the National Academy of Sciences*, 116, 7916–7925.

Olson, M.E., & Arroyo-Santos, A. (2009). Thinking in continua: Beyond the “adaptive radiation” metaphor. *BioEssays*, 31, 1337–1346. <https://doi.org/10.1002/bies.200900102>

Pagel, M. (1999). Inferring the historical patterns of biological evolution. *Nature*, 401, 877–884. <https://doi.org/10.1038/44766>

Pagel, M., O'Donovan, C., & Meade, A. (2022). General statistical model shows that macroevolutionary patterns and processes are consistent with Darwinian gradualism. *Nature Communications*, 13, 1113. <https://doi.org/10.1038/s41467-022-28595-z>

Pavlicev, M., Cheverud, J.M., & Wagner, G.P. (2009). Measuring morphological integration using eigenvalue variance. *Evolutionary Biology*, 36, 157–170. <https://doi.org/10.1007/s11692-008-9042-7>

Pennell, M.W., Eastman, J.M., Slater, G.J., Brown, J.W., Uyeda, J.C., FitzJohn, R.G., Alfaro, M.E., & Harmon, L.J. (2014). geiger v2.0: An expanded suite of methods for fitting macroevolutionary models to phylogenetic trees. *Bioinformatics*, 30, 2216–2218. <https://doi.org/10.1093/bioinformatics/btu181>

Pigot, A.L., Trisos, C.H., & Tobias, J.A. (2016). Functional traits reveal the expansion and packing of ecological niche space underlying an elevational diversity gradient in passerine birds. *Proceedings of the Royal Society B: Biological Sciences*, 283, 20152013. <https://doi.org/10.1098/rspb.2015.2013>

Polly, P.D., Lawing, A.M., Fabre, A.-C., & Goswami, A. (2013). Phylogenetic principal components analysis and geometric morphometrics. *Hystrix*, 24, 33–41.

Rabosky, D.L., Santini, F., Eastman, J., Smith, S.A., Sidlauskas, B., Chang, J., & Alfaro, M.E. (2013). Rates of speciation and morphological evolution are correlated across the largest vertebrate radiation. *Nature Communications*, 4, 1958. <https://doi.org/10.1038/ncomms2958>

Reaney, A.M., Bouchenak-Khelladi, Y., Tobias, J.A., & Abzhanov, A. (2020). Ecological and morphological determinants of evolutionary diversification in Darwin's finches and their relatives. *Ecology and Evolution*, 10, 14020–14032. <https://doi.org/10.1002/ece3.6994>

Reddy, S., & Schulenberg, T.S. (2022). *The new natural history of Madagascar*. Princeton University Press.

Reddy, S., Driskell, A., Rabosky, D.L., Hackett, S.J., & Schulenberg, T.S. (2012). Diversification and the adaptive radiation of the vangas of Madagascar. *Proceedings of the Royal Society B: Biological Sciences*, 279, 2062–2071. <https://doi.org/10.1098/rspb.2011.2380>

Revell, L.J. (2009). Size-correction and principal components for interspecific comparative studies. *Evolution*, 63, 3258–3268. <https://doi.org/10.1111/j.1558-5646.2009.00804.x>

Roberts-Hugghis, A.S., Burress, E.D., Lam, B., & Wainwright, P.C. (2023). The cichlid pharyngeal jaw novelty enhances evolutionary integration in the feeding apparatus. *Evolution*, 77, 1917–1929. <https://doi.org/10.1093/evolut/qpad109>

Rohlf, F.J., & Slice, D. (1990). Extensions of the Procrustes method for the optimal superimposition of landmarks. *Systematic Biology*, 39, 40–59.

Rowsey, D.M., Heaney, L.R., & Jansa, S.A. (2019). Tempo and mode of mandibular shape and size evolution reveal mixed support for incumbency effects in two clades of island-endemic rodents (Muridae:Murinae)\*. *Evolution*, 73, 1411–1427. <https://doi.org/10.1111/evo.13737>

Rowsey, D.M., Keenan, R.M., & Jansa, S.A. (2020). Dietary morphology of two island-endemic murid rodent clades is consistent with persistent, incumbent-imposed competitive interactions. *Proceedings of the Royal Society B: Biological Sciences*, 287, 20192746. <https://doi.org/10.1098/rspb.2019.2746>

Rundell, R.J., & Price, T.D. (2009). Adaptive radiation, nonadaptive radiation, ecological speciation and nonecological speciation. *Trends in Ecology & Evolution*, 24, 394–399. <https://doi.org/10.1016/j.tree.2009.02.007>

Safford, R., & Hawkins, F. (2013). *The birds of Africa: Volume VIII: The Malagasy region: Madagascar, Seychelles, Comoros, M ascarenes*. A&C Black.

Schlüter, D. (1996). Adaptive radiation along genetic lines of least resistance. *Evolution*, 50, 1766–1774. <https://doi.org/10.2307/2410734>

Schlüter, D. (2000). *The ecology of adaptive radiation*. Oxford University Press. <https://doi.org/10.1093/oso/9780198505235.001.0001>

Seehausen, O. (2004). Hybridization and adaptive radiation. *Trends in Ecology & Evolution*, 19, 198–207. <https://doi.org/10.1016/j.tree.2004.01.003>

Sidlauskas, B. (2008). Continuous and arrested morphological diversification in sister clades of characiform fishes: A phylogenospace approach. *Evolution*, 62, 3135–3156. <https://doi.org/10.1111/j.1558-5646.2008.00519.x>

Silvestro, D., Kostikova, A., Litsios, G., Pearman, P.B., & Salamin, N. (2015). Measurement errors should always be incorporated in phylogenetic comparative analysis. *Methods in Ecology and Evolution*, 6, 340–346. <https://doi.org/10.1111/2041-210X.12337>

Simpson, G.G. (1944). *Tempo and mode in evolution*. Columbia University Press.

Slater, G.J. (2022). Topographically distinct adaptive landscapes for teeth, skeletons, and size explain the adaptive radiation of Carnivora (Mammalia). *Evolution*, 76, 2049–2066. <https://doi.org/10.1111/evol.14577>

Slater, G.J., & Friscia, A.R. (2019). Hierarchy in adaptive radiation: A case study using the Carnivora (Mammalia). *Evolution*, 73, 524–539. <https://doi.org/10.1111/evo.13689>

Slater, G.J., & Pennell, M.W. (2014). Robust regression and posterior predictive simulation increase power to detect early bursts of trait evolution. *Systematic Biology*, 63, 293–308. <https://doi.org/10.1093/sysbio/syt066>

Slater, G.J., Price, S.A., Santini, F., & Alfaro, M.E. (2010). Diversity versus disparity and the radiation of modern cetaceans. *Proceed-*

ings of the Royal Society B: Biological Sciences, 277, 3097–3104. <https://doi.org/10.1098/rspb.2010.0408>

**Starr, K.B.**, Sherratt, E., & Sanger, T.J. (2024). Large morphological transitions underlie exceptional shape diversification in an adaptive radiation. *Scientific Reports*, 14, 31884. <https://doi.org/10.1038/s41598-024-83404-5>

**Stratovan Corporation.** (2018). Stratovan Checkpoint. [stratovan.com/products/checkpoint](http://stratovan.com/products/checkpoint). Date accessed June 7, 2024.

**Stroud, J.T.**, & Losos, J.B. (2016). Ecological opportunity and adaptive radiation. *Annual Review of Ecology, Evolution, and Systematics*, 47, 507–532. <https://doi.org/10.1146/annurev-ecolsys-121415-032254>

**Tobias, J.A.**, Sheard, C., Pigot, A.L., Devenish, A.J.M., Yang, J., Sayol, F., Neate-Clegg, M.H.C., Alioravainen, N., Weeks, T.L., Barber, R.A., Walkden, P.A., MacGregor, H.E.A., Jones, S.E.I., Vincent, C., Phillips, A.G., Marples, N.M., Montaño-Centellas, F.A., Leandro-Silva, V., Claramunt, S., & Schleuning, M. (2022). AVONET: Morphological, ecological and geographical data for all birds. *Ecology Letters*, 25, 581–597. <https://doi.org/10.1111/ele.13898>

**Troyer, E.M.**, Evans, K.M., Goatley, C.H.R., Friedman, M., Carnevale, G., Nicholas, B., Kolmann, M., Bemis, K.E., & Arcila, D. (2024). Evolutionary innovation accelerates morphological diversification in pufferfishes and their relatives. *Evolution*, 78, 1869–1882. <https://doi.org/10.1093/evolut/qpae127>

**Uyeda, J.C.**, Caetano, D.S., & Pennell, M.W. (2015). Comparative analysis of principal components can be misleading. *Systematic Biology*, 64, 677–689. <https://doi.org/10.1093/sysbio/syv019>

**van der Meij, M.A.A.**, & Bout, R.G. (2008). The relationship between shape of the skull and bite force in finches. *Journal of Experimental Biology*, 211, 1668–1680. <https://doi.org/10.1242/jeb.015289>

**Venditti, C.**, Meade, A., & Pagel, M. (2011). Multiple routes to mammalian diversity. *Nature*, 479, 393–396. <https://doi.org/10.1038/nature10516>

**Vinciguerra, N.T.**, & Burns, K.J. (2021). Species diversification and ecomorphological evolution in the radiation of tanagers (Passeriformes: Thraupidae). *Biological Journal of the Linnean Society*, 133, 920–930. <https://doi.org/10.1093/biolinнейn/blab042>

**Wagner, G.P.**, & Altenberg, L. (1996). Perspective: Complex adaptations and the evolution of evolvability. *Evolution*, 50, 967–976. <https://doi.org/10.2307/2410639>

**Walter, G.M.**, Aguirre, J.D., Blows, M.W., & Ortiz-Barrientos, D. (2018). Evolution of genetic variance during adaptive radiation. *The American Naturalist*, 191, E108–E128. <https://doi.org/10.1086/696123>

**Wellborn, G.A.**, & Langerhans, R.B. (2015). Ecological opportunity and the adaptive diversification of lineages. *Ecology and Evolution*, 5, 176–195. <https://doi.org/10.1002/ece3.1347>

**Wilmé, L.** (1996). Composition and characteristics of bird communities in Madagascar. *Biogéographie de Madagascar*. ORSTOM, Paris. 349–362.

**Wogan, G.O.U.**, Yuan, M.L., Mahler, D.L., & Wang, I.J. (2023). Hybridization and transgressive evolution generate diversity in an adaptive radiation of anolis lizards. *Systematic Biology*, 72, 874–884. <https://doi.org/10.1093/sysbio/syad026>

**Yamagishi, S.**, & Eguchi, K. (1996). Comparative foraging ecology of Madagascar vangids (Vangidae). *IBIS*, 138, 283–290. <https://doi.org/10.1111/j.1474-919X.1996.tb04340.x>

**Yamagishi, S.**, Honda, M., Eguchi, K., & Thorstrom, R. (2001). Extreme endemic radiation of the Malagasy vangas (Aves: Passeriformes). *Journal of Molecular Evolution*, 53, 39–46. <https://doi.org/10.1007/s002390010190>

**Yang, A.S.** (2001). Modularity, evolvability, and adaptive radiations: A comparison of the hemi- and holometabolous insects. *Evolution & Development*, 3, 59–72. <https://doi.org/10.1046/j.1525-142x.2001.003002059.x>

**Yoder, J.B.**, Clancey, E., Des Roches, S., Eastman, J.M., Gentry, L., Godsoe, W., Hagey, T.J., Jochimsen, D., Oswald, B.P., Robertson, J., Sarver, B.A.J., Schenk, J.J., Spear, S.F., & Harmon, L.J. (2010). Ecological opportunity and the origin of adaptive radiations. *Journal of Evolutionary Biology*, 23, 1581–1596. <https://doi.org/10.1111/j.1420-9101.2010.02029.x>

**Younger, J.L.**, Dempster, P., Nyári, Á.S., Helms, T.O., Raherilalao, M.J., Goodman, S.M., & Reddy, S. (2019). Phylogeography of the Rufous Vanga and the role of bioclimatic transition zones in promoting speciation within Madagascar. *Molecular Phylogenetics and Evolution*, 139, 106535. <https://doi.org/10.1016/j.ympev.2019.106535>

**Zelditch, M.L.**, & Goswami, A. (2021). What does modularity mean? *Evolution & Development*, 23, 377–403. <https://doi.org/10.1111/ede.12390>

**Zelditch, M.L.**, Swiderski, D.L., & Sheets, H.D. (2012). *Geometric morphometrics for biologists: A primer*. Academic Press.

**Zusi, R.L.** (1993). *The skull, volume 2: Patterns of structural and systematic diversity*. University of Chicago Press.